Fluid closures: the introduction of kinetic effects

Thierry Passot
UNS, CNRS, Observatoire de la Côte d'Azur, Nice, France

Collaborators:
D. Borgogno, P. Henri, P. Hunana, D. Laveder, L. Marradi, and P.L. Sulem

The future of plasma astrophysics: Combining experiments, observations, simulations and theory

Ecole de Physique des Houches, France
25 february- 8 march 2013

Research supported in part by the European Commission's 7th Framework Program (PF7:2007-2013) under grant agreement SHOCK (project # 284515) and Programme Terre-Soleil of INSU-CNRS.

SHOCK.
SOLAR AND HELIOSPHERIC COLLISIONLESS KINETICS

Outline

- The solar wind context: Importance of compressibility, dispersion, temperature anisotropy, kinetic effects
- The fluid approach: from incompressible MHD to the Landau fluid model
- The FLR Landau fluid model: properties of the linear system
- Other validations of the model
- 3D decay simulations
- 1D driven simulations at quasi-perpendicular angle
- Conclusions

Main features of Space plasmas

Space plasmas are magnetized and turbulent with essentially no collision.

$\beta \approx 1$, $M_s \approx 1$

Fluctuations: power-law spectra
extend to ion gyroscale and below

Dispersive and kinetic effects cannot be ignored.

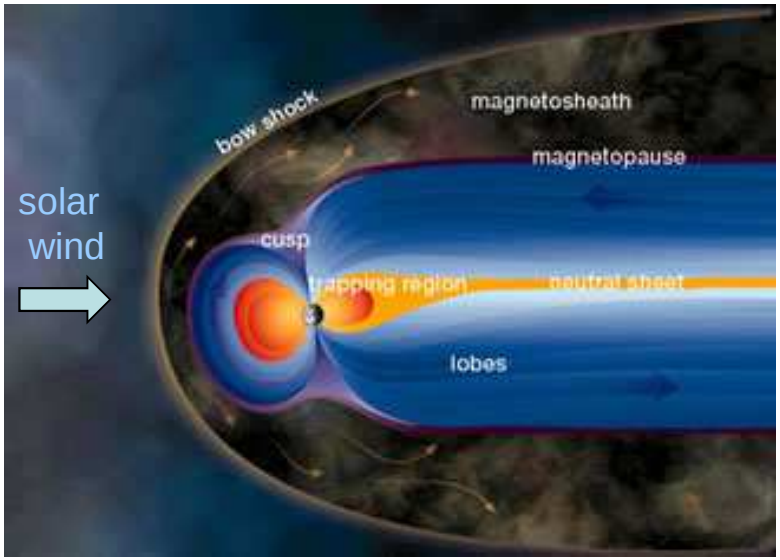

Presence of coherent structures (filaments, shocklets, magnetosonic solitons, magnetic holes) with typical scales of a few ion Larmor radii.

The concepts of waves make sense even in the strong turbulence regime

Space plasmas: debated questions

1. Spectral energy distribution and its anisotropy in the solar wind

Excess of magnetic energy in the transverse components

Several power-law ranges: Are they cascades? which waves? which slopes? Important to estimate the heating rates.

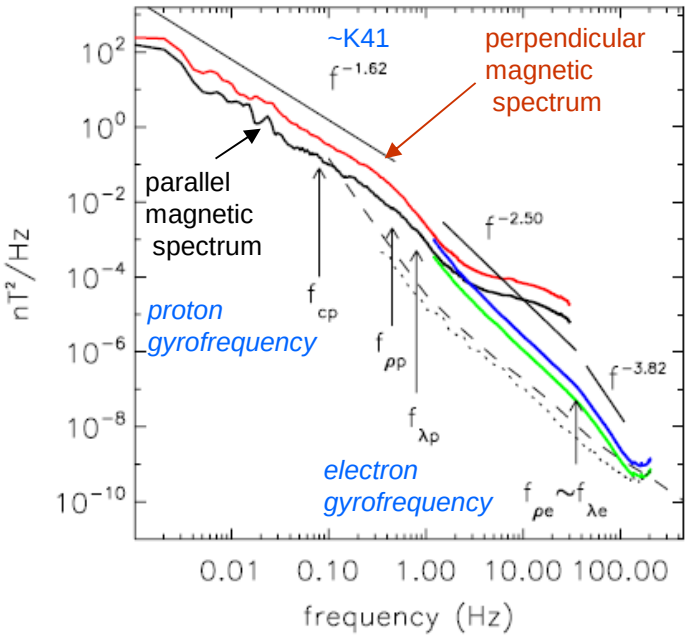

Sahraoui et al. PRL 102, 231102 (2009)

k-filtering -> θ=86°

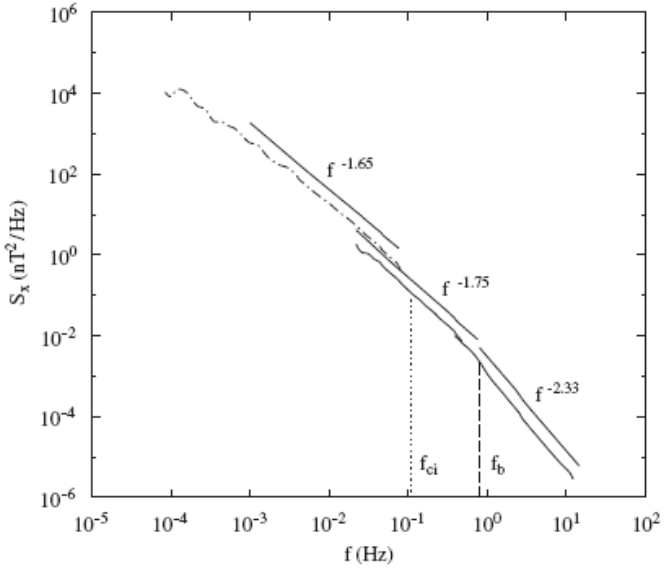

Alexandrova et al. Planet. Space Sci. 55, 2224 (2007)

Does the anisotropy persist at small scales?

At what scale does dissipation take place?
By which mechanism?
Role of ion and electron Landau damping ?

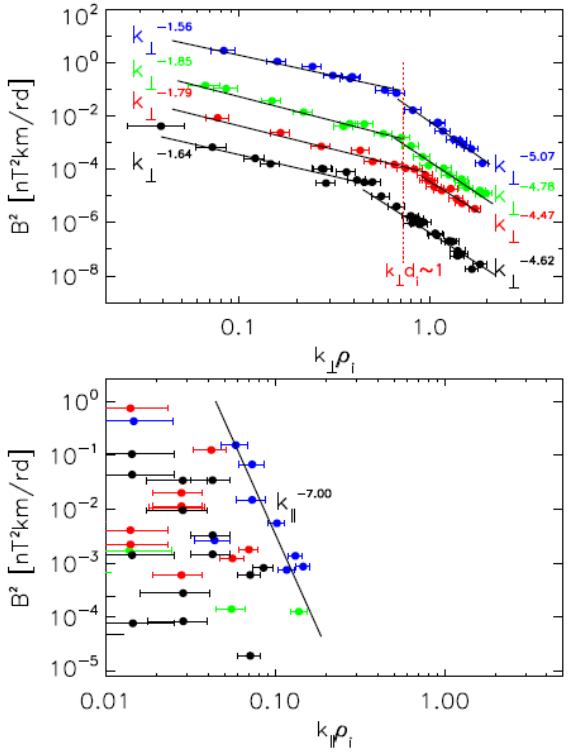

Heating of protons via Landau damping ?

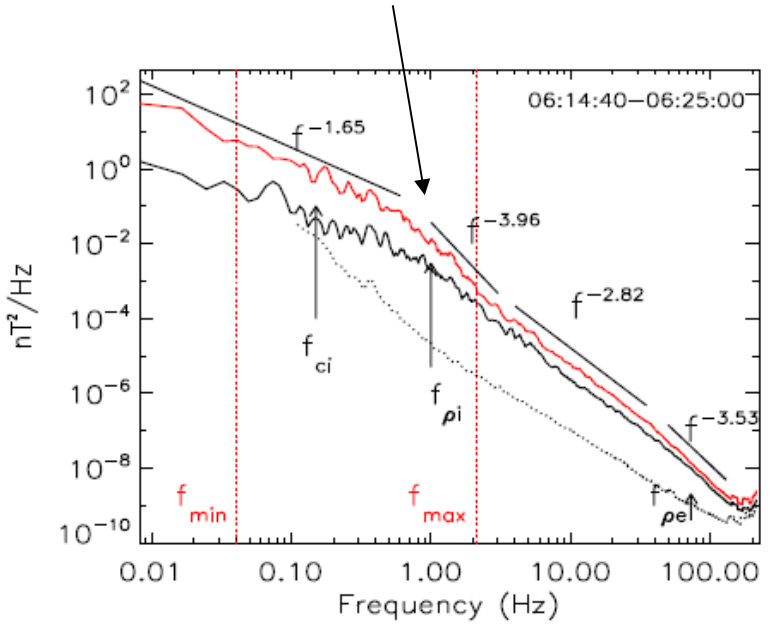

From Sahraoui et al. PRL (2010).

2. Main features of Terrestrial magnetosheath plasma

Important role of the temperature anisotropy:
AIC (near quasi-perpendicular shock) and mirror instabilities (further inside magnetosheath)

Domination of mirror modes
spatial spectrum steeper than temporal one

Here identified as mirror modes using k-filtering technique (*Pinçon & Lefeuvre, JGR 96, 1789; 1991*):
modes with essentially zero frequency in the plasma frame

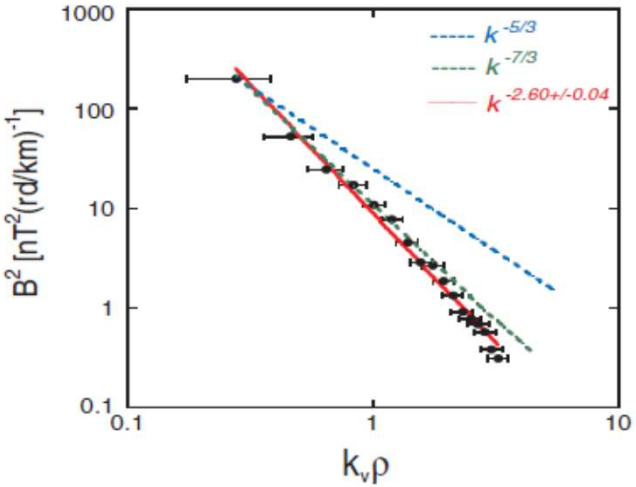

Sahraoui et al. PRL 2006

and of coherent structures:

- Current filaments
- Mirror structures (magnetic holes and humps)

Drift Kinetic Alfvén Vortices also observed in the cusp region.
(*Sundkvist et al. Nature, Aug.; 2005*)

Alfvén vortices

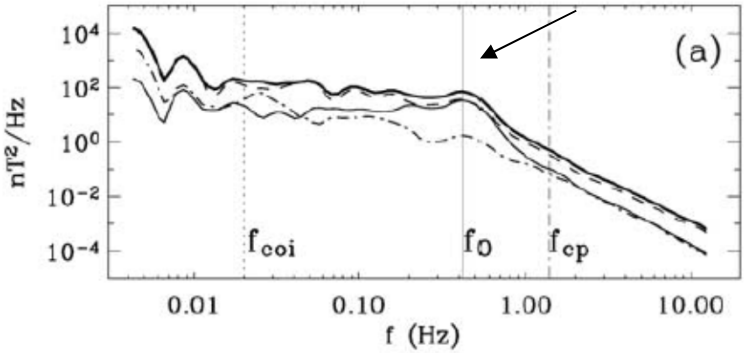

Alexandrova et al. JGR 111, A12208 (2006).

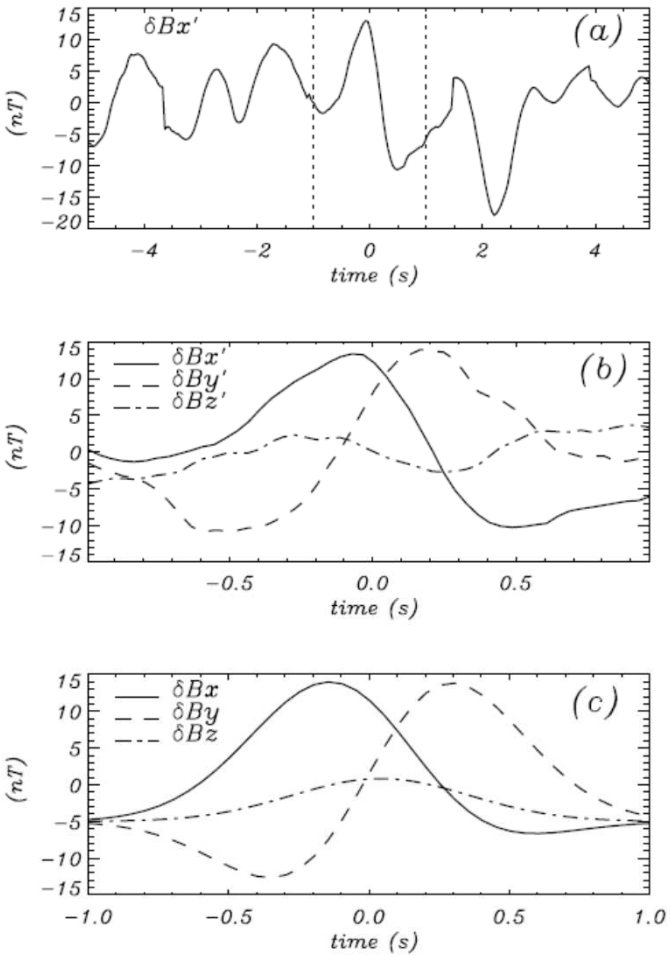

Figure 8. Magnetic field fluctuations, taking $\tau \simeq -420$ s (1755:16 UT) as the origin of time. (a) Fluctuations $\delta B_{x'}$ during 10 s around τ. (b) Fluctuations of the magnetic field components ($\delta B_{x'}$, $\delta B_{y'}$, $\delta B_{z'}$) for the 2-s period around τ. (c) The z-aligned current tube simulation (δB_x, δB_y, δB_z).

Signature of magnetic filaments
(Alexandrova et al. JGR 2004)

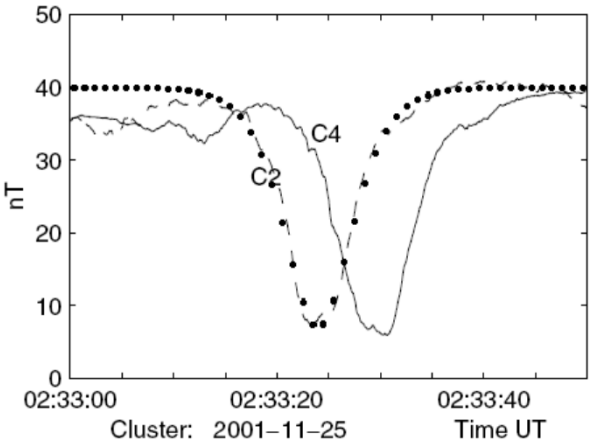

FIG. 1. A large scale soliton observed by Cluster spacecraft C2 (dashed) and C4 (solid) in the total magnetic field. Marked curve shows fit of $b_0\,\mathrm{sech}^2[(t-t_0)/\delta t]$ with $b_0 = -33$ nT and $\delta t = 4.4$ s. The soliton moves with velocity $u_0 \approx 250$ km/s and has a width of 2000 km. The position of Cluster satellites was $(-4, 17, 5)\ R_E$ GSE.

Slow magnetosonic solitons
(Stasiewicz et al. PRL 2003)

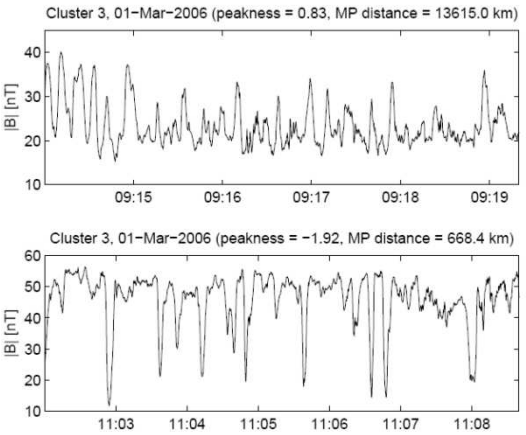

Mirror structures in the terrestrial magnetosheath
(Soucek et al.JGR 2008)

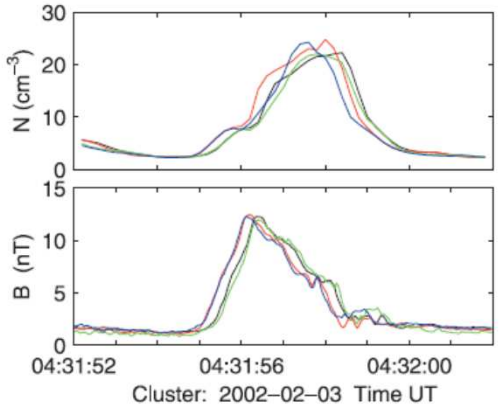

Figure 2. Pulse-like enhancements of the plasma density and magnetic field measured on four Cluster spacecraft: C1–C4, which are color coded in sequence: black, red, green, blue. The measurements represent signatures of fast magnetosonic shocklets moving with supersonic speed in a high-β plasma.

Fast magnetosonic shocklets
(Stasiewicz et al. GRL 2003)

2. Heating of the plasma: temperature anisotropy and resulting micro-instabilities

Turbulence (and/or solar wind expansion) generate temparature anisotropy
This anisotropy is limited by mirror and oblique firehose instabilities.
Role of anisotropy on the turbulence « dissipative range»?

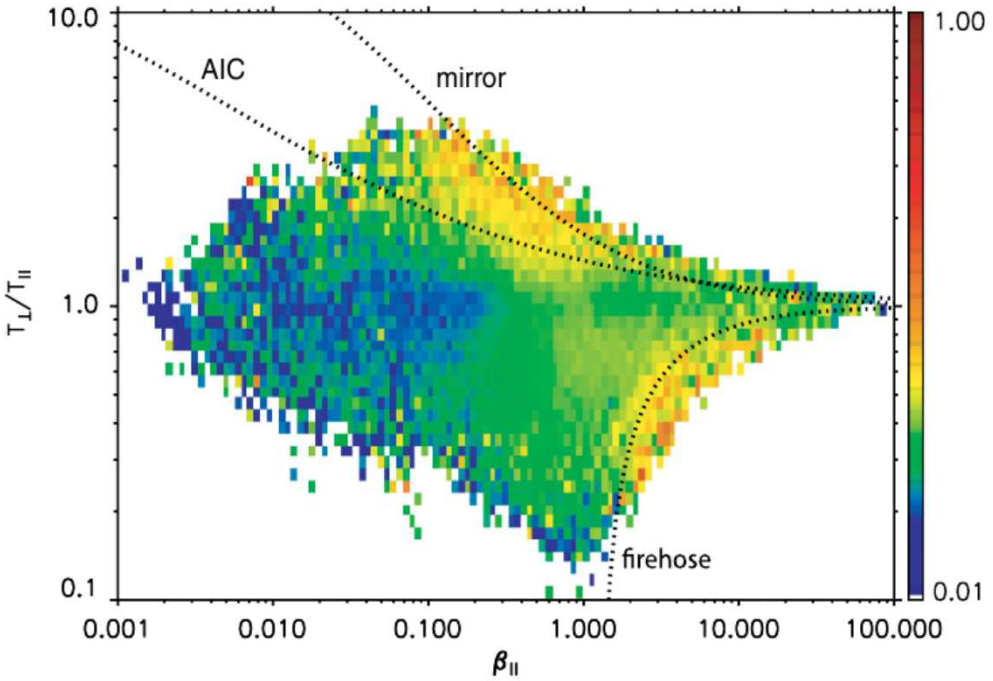

Bale et al. PRL 103, 21101 (2009);
see also Hellinger et al. GRL 33, L09101 (2006).

color: magnitude of δB; enhanced δB also corresponds to enhanced proton heating.

How to construct a fluid model for collisionless plasmas ?

One needs a fluid model that

- retains low-frequency kinetic effects: Landau damping and FLR corrections
- can be integrated relatively fast
- allows for strong temperature anisotropies
- does not a priori order out the fast magnetosonic waves.

Requirements: The model should

- reproduce the linear properties of low-frequency waves.
- ensure that the system does not develop spurious instabilities at scales smaller than its range of validity, and thus remains well-posed in the nonlinear regime.

Such a fluid model could also prove useful to provide initial and/or boundary conditions for Vlasov simulations.

The various fluid approaches

Incompressible MHD

Drastic approximation, that assumes the presence of collisions; valid at very large scales.
Allows one to focus mainly on nonlinear phenomena.

Still many open problems:

The turbulent regime is not totally understood (see Boldyrev's lecture)
(various theories : *Iroshnikov-Kraichnan 1965, Goldreich-Sridhar 1995, Perez & Boldyrev 2009*).

This model has many advantages:

Possibility to identify two conserved quantities ($\int (z^{\pm})^2$ where $z^{\pm} = u \pm b$)
which separately cascade towards small scales.

Existence of an exact law, analogous to the 4/5 law of Karman-Howarth
for homogeneous isotropic turbulence, giving statistics of 3rd order moments for velocity increments (*Politano & Pouquet, GRL 25, 273; 1998*) and allowing
for the estimation of turbulent heating (Sorriso-Valvo et al. PRL **99,** 115001 (2007))

Reduced MHD

In the presence of a strong ambient field, the dynamics is essentially decoupled, even for finite beta, between:

- Incompressible MHD in the planes transverse to B_0
- Alfvén waves parallel to B_0

Reduced MHD can be derived from gyrokinetic theory (Schekochihin, ApJ. sup. 2009).

To account for « temporal » dispersive effects at scales of the order or smaller than d_i:

Hall MHD

Replace Ohm's law E=-U x B by a more general expression.
After taking electron velocity equation, neglecting electron inertia, write:

$$\mathbf{E} + \mathbf{U} \times \mathbf{B} - \frac{1}{n_e e}\mathbf{J} \times \mathbf{B} + \frac{1}{n_e e}\nabla\left(n_e \kappa T_e\right) = \eta \mathbf{J}$$

If diffusive term and electron pressure are neglected:

$$E=-U_e \times B$$

Decoupling of electron and ion velocities.
The magnetic field however remains frozen in the electron flow.

With an ambient field and in the linear approximation: dispersive effects lead to separation of AWs into whistlers and ion cyclotron modes.

Incompressible limit only valid only in the limit $\beta \to \infty$ (Sahraoui et al. JPP '07)

In the dispersive case, it is possible to derive a 4/5 law (*Galtier, PRE 77, 015302 (R); 2008*) and to develop a theory of weak turbulence (Galtier, JPP 2006).

Both in the weak turbulence regime and in a shell model (Galtier and Buchlin ApJ 2007), incompressible Hall-MHD is able to capture a transition from an AW cascade at large scale, towards another type of cascade dominated by the Hall nonlinearity.

Transition at the ion inertial length: $d_i = v_A/\Omega$

In order to capture finite beta effects:

The compressible Hall-MHD model

$$\partial_t \rho + \nabla.(\rho \mathbf{u}) = 0$$

$$\rho(\partial_t \mathbf{u} + \mathbf{u}.\nabla \mathbf{u}) = -\frac{\beta}{\gamma}\nabla \rho^\gamma + (\nabla \times \mathbf{b}) \times \mathbf{b}$$

$$\partial_t \mathbf{b} - \nabla \times (\mathbf{u} \times \mathbf{b}) = -\underbrace{\frac{1}{R_i}\nabla \times (\frac{1}{\rho}(\nabla \times \mathbf{b}) \times \mathbf{b})}_{\text{Hall term}}$$

$$\nabla.\mathbf{b} = 0$$

In the presence of an ambient field, the Hall term induces dispersive effects.

Hall-MHD is a rigorous limit of collisionless kinetic theory for:

cold ions:

$T_i << T_e$
$\omega << \Omega_i$
$k_{||}\, v_{thi} << \omega << k_{||}\, v_{the}$

Irose et al. , Phys. Lett. A 330, 474 (2004)
Ito et al., PoP 11, 5643 (2004)
Howes, NPG 16, 219 (2009)

It correctly reproduces whistlers and KAW's for small to moderate β.

➔ *It contains waves that are usually damped in a collisionless plasma and whose influence in the turbulent dynamics has to be evaluated.*

Compressibility introduces coupling to magnetosonic modes and allows for the presence of the decay instability for β<1: important for the generation of contra-propagating Alfvén waves and thus the development of a cascade.

Dispersion can lead to solitonic structures:

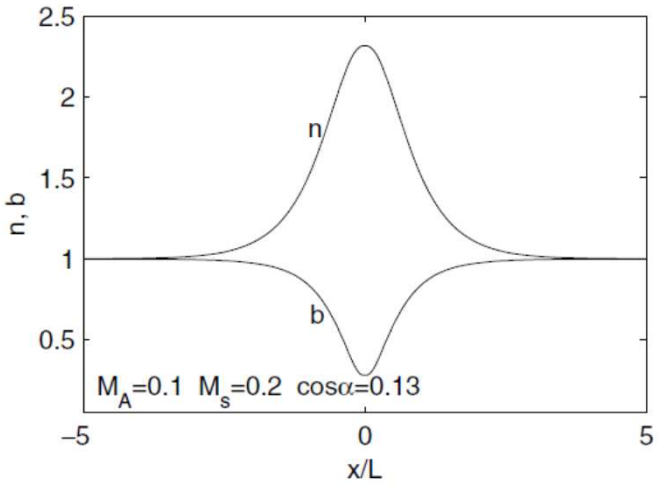

Oblique soliton in Hall-MHD
(from Stasiewicz et al. PRL 2003)

but can also be the source of modulational instabilities and the formation of small scales: wave collapse:

Example: Alfvén wave filamentation in 3D Hall-MHD:

$|B_\perp|$

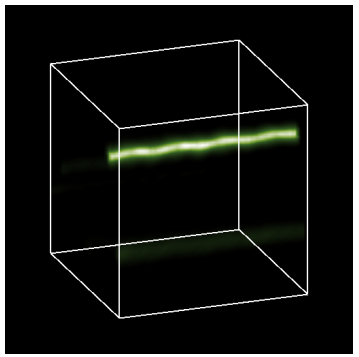

Laveder et al. PoP 9, 293; 2002

But compressible Hall-MHD lacks finite Larmor radius corrections, important for β~1, and the correct dissipation of slow modes.

In order to capture high frequency phenomena and to break the magnetic field frozen-in condition: Introduce electron inertia.

The bifluid model

Dynamical equations for the electron velocity.

Allows one to study:

- whistler turbulence
(neglecting ion inertia the model can be simplified to so-called electron MHD;
at small scales: ions are essentially immobile; currents are due to electrons)

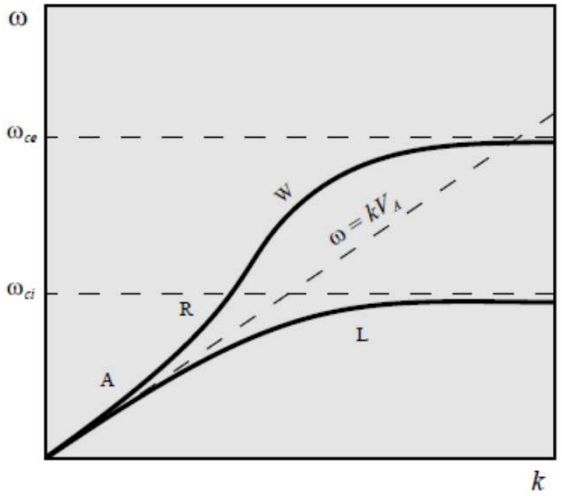

Figure 8.12 Modes R et L ioniques : onde d'Alfvén.

From Rax, Physique des Plasmas

- reconnection
no need to introduce dissipative mechanisms;
fast collisionless reconnection

Relax the collisionallity assumption: introduce a tensorial pressure and the so-called:

Chew Goldberger Law (CGL) model or double adiabatic law

Chew et al., Proc. R. Soc. London A **236**, 112 , 1956

Assume a simple Ohm's law without Hall term and electron pressure gradient, and zero heat fluxes

Gyrotropy; tensor in the local frame: $\overleftrightarrow{\mathbf{P}}^{\mathrm{MHD}} = \begin{bmatrix} P_\perp & 0 & 0 \\ 0 & P_\perp & 0 \\ 0 & 0 & P_\parallel \end{bmatrix} = P_\perp \overleftrightarrow{\mathbf{I}} + (P_\parallel - P_\perp)\hat{\mathbf{B}}\hat{\mathbf{B}}$

Conservation of adiabatic invariants:

$$\frac{P_\parallel B^2}{\rho^3} = const. \qquad \frac{P_\perp}{\rho B} = const.$$ along flow trajectories

The adiabatic closure assumes that wave phase speeds are much larger than particles thermal velocities : it is not a proper closure for the solar wind.

For large enough temperature anisotropies, existence of instabilities.

Problem: CGL leads to wrong mirror threshold and does not provide stabilization at small scales

Polytropic laws are in general invalid.

Generalized polytropic indices for wave modes (Belmont & Mazelle JGR 97, 8327 (1992):

$$\gamma_{//} = 2\xi^2 - \frac{2}{Z'} + \frac{1}{C_P}\left[1 - \left(2\xi^2 - \frac{2}{Z'}\right)\right]$$

$$\gamma_{\perp} = 1 + \frac{1}{C_P}\left[1 + \frac{Z'}{2}(1 - A)\right]$$

$$C_P = \frac{n^1/n}{B^1/B}$$ is the compressibility

$$\xi = \omega/\sqrt{2}k_{//}V_{//}$$

Z is the plasma dispersion function

$A = 1 - T_{\perp}/T_{//}$ is the anisotropy

Adiabatic limit (CGL) $\xi >> 1$

$$\gamma_{//} = 3 - \frac{2}{C_P}$$

$$\gamma_{\perp} = 1 + \frac{1}{C_P}$$

Isothermal limit $\xi << 1$

$$\gamma_{//} = 1 + \frac{i\sqrt{\pi}\,\xi}{C_P}$$

$$\gamma_{\perp} = 1 + \frac{A - i\sqrt{\pi}\,\xi(1-A)}{C_P}$$

For mirror modes e.g. ξ is to be kept.

Depend on the mode; fit well the data. Can lead to closure relations independent of plasma modes, for linear variations, but of differential type.

A MHD-like model for steady mirror structures

Although the mirror instability is driven by kinetic effects, some properties of stationary mirror structures can be captured within the anisotropic MHD, supplemented with a suitable equations of state.

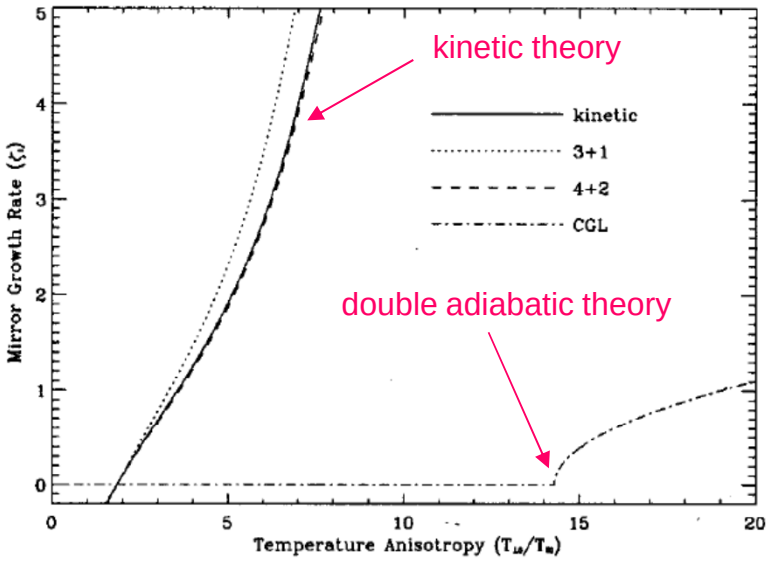

FIG. 5. The linear growth rate of the mirror instability ($k_\perp^2 \gg k_\parallel^2$) as predicted by kinetic theory, 3+1 and 4+2 Landau MHD models, and CGL theory (ideal MHD cannot predict the mirror growth rate as it posits an isotropic pressure). The normalized growth rate $[\zeta_i = \mathrm{Im}(\omega)/\sqrt{2}|k_\parallel| v_{T_{\parallel_i}}]$ is plotted versus the temperature anisotropy $(T_{\perp_0}/T_{\parallel_0})$ at constant $\beta = \{(2/3)p_{\perp_0} + (1/3)p_{\parallel_0}\}/(B_0^2/8\pi)$. The parameters chosen are $Z=1$, $T_{\perp_{0i}} = T_{\perp_{0e}}$, $T_{\parallel_{0i}} = T_{\parallel_{0e}}$, $\beta = 1$, and $\sqrt{m_i/m_e} = 40$.

Snyder et al., PoP **4**, 3974 (1997)

CGL is **NOT appropriate** for mirror modes (that are static in the plasma frame).

Ad hoc anisotropic polytropic equations of state with parallel and perpendicular indices chosen in such a way that the mirror instability threshold is reproduced, have been considered

(Hau et al., PoP **12**, 122904, 2005; NPG **14**, 557, 2007 and reference therein).

An **isothermal** or **static limit** is more suitable for mirror modes.

A series of equations can be derived for the gyrotropic components of the even moments, and using the assumption of bi-Maxwellian distributions, simple equations of state can be obtained, which predicts the **correct threshold of the mirror instability.**

Model potentially relevant for describing the large-scale features of steady mirror structures:

Indeed,

- **Landau damping vanishes for static solutions.**
- **FLR corrections negligible at large scales.**

Landau damping and FLR corrections are needed in order to reproduce the correct instability growth rate.

Consider the **static regime** characterized by a zero hydrodynamic velocity and no time dependency of the other moments (Passot, Ruban and Sulem, PoP **13**, 102310, 2006).

Assume cold electrons (no parallel electric field)

Projecting the ion velocity equation along the local magnetic field (whose direction is defined by the unit vector $\hat{b}$) leads to the parallel pressure equilibrium condition

$$\hat{b}_m \frac{\partial}{\partial x_n} P_{mn} = 0$$

for the (gyrotropic) pressure tensor $P_{ij} = p_\perp n_{ij} + p_\parallel \tau_{ij}$

where $n_{ij} = \delta_{ij} - \hat{b}_i \hat{b}_j$ and $\tau_{ij} = \hat{b}_i \hat{b}_j$ are the fundamental gyrotropic tensors.

The above condition rewrites: $(\hat{b} \cdot \nabla) p_\parallel + (p_\parallel - p_\perp) \nabla \cdot \hat{b} = 0.$

From the divergenceless of **B** = B $\hat{b}$, one has $\frac{1}{\nabla \cdot \hat{b}} \hat{b} \cdot \nabla = - \frac{B}{\hat{b} \cdot \nabla B} \hat{b} \cdot \nabla = - \bar{B} \frac{d}{d\bar{B}} = - \frac{d}{dX},$

with $\boxed{X = \ln \bar{B}.}$

This leads to the condition $\boxed{\frac{dp_\parallel}{dX} = p_\parallel - p_\perp .}$

We proceed in a similar way at the level of the equation for the heat flux tensor, by contracting with the two fundamental tensors τ_{ij} and n_{ij}, and get

$$\hat{b}_l \tau_{ij} \frac{\partial}{\partial x_k} R_{ijkl} = 0,$$

$$\hat{b}_l n_{ij} \frac{\partial}{\partial x_k} R_{ijkl} = 0,$$

where the 4th-order moment is taken in the gyrotropic form

$$R_{ijkl} = r_{\parallel\parallel} \tau_{ij} \tau_{kl} + r_{\parallel\perp} \mathcal{S}\{n_{ij} \tau_{kl}\} + r_{\perp\perp} \mathcal{S}\{n_{ij} n_{kl}\}.$$

Here, $\mathcal{S}$ refers to the symmetrization with respect to all the indices. One gets

$$\frac{dr_{\parallel\parallel}}{dX} = r_{\parallel\parallel} - 3r_{\parallel\perp},$$

$$\frac{dr_{\parallel\perp}}{dX} = 2r_{\parallel\perp} - r_{\perp\perp}.$$

The **closure** then consists in assuming that the 4th-order moments are related to the second order ones as in the case of a bi-Maxwellian distribution, i.e.:

$$r_{\parallel\parallel} = 3p_{\parallel}^2/\rho \qquad r_{\parallel\perp} = p_{\parallel}p_{\perp}/\rho \qquad \text{and} \qquad r_{\perp\perp} = 2p_{\perp}^2/\rho$$

Closure can be done at higher order

One finally gets

$$\begin{cases} \dfrac{d\bar{T}_{\parallel}}{dX} = 0, \\ \dfrac{d\bar{T}_{\perp}}{dX} = \bar{T}_{\perp}\left[1 - (A+1)\dfrac{\bar{T}_{\perp}}{\bar{T}_{\parallel}}\right]. \end{cases}$$

These equations are solved as

$$\bar{T}_{\parallel} = 1, \qquad \bar{T}_{\perp} = \frac{\bar{B}}{(A+1)\bar{B} - A}$$

$$A = (T_{\perp}^{(0)}/T_{\parallel}^{(0)}) - 1$$

« Initial condition » at X=0

Similar equations of state were derived using a fully kinetic argument by Constantinescu, J. Atmos. Terr. Phys. **64**, 645 (2002).

Equations actually also valid with warm electrons

This is exactly the same closure as the one introduced in Belmont's lecture (in flux tube).

Kinetic MHD

(« *MHD description of plasma* » by R.M. Kulsrud)

Handbook of Plasma Physics, Eds. M.N. Rosenbluth and R.Z. Sagdeev
Volume 1: Basic Plasma Physics I, edited by A.A. Galeev and R.N. Sudan

$$\partial\rho/\partial t + \nabla\cdot(\rho \boldsymbol{U}) = 0,$$

$$\rho\left(\frac{\partial \boldsymbol{U}}{\partial t} + \boldsymbol{U}\cdot\nabla\boldsymbol{U}\right) = \frac{(\nabla\times\boldsymbol{B})\times\boldsymbol{B}}{4\pi} - \nabla\cdot\boldsymbol{P},$$

$$\partial\boldsymbol{B}/\partial t = \nabla\times(\boldsymbol{U}\times\boldsymbol{B}),$$

$$\boldsymbol{P} = p_\perp \boldsymbol{I} + (p_\parallel - p_\perp)\boldsymbol{bb},$$

$$p_\perp = \sum_s m_s \int f_{0s}\frac{v_\perp^2}{2}\,\mathrm{d}^3v,$$

$$p_\parallel = \sum_s m_s \int f_{0s}(v_\parallel - \boldsymbol{U}\cdot\boldsymbol{b})^2\,\mathrm{d}^3v,$$

$$\frac{\partial f_{0s}}{\partial t} + (\boldsymbol{U}_\mathrm{E} + v_\parallel \boldsymbol{b})\cdot\nabla f_{0s} - v_\perp\left(\nabla\cdot\boldsymbol{U}_\perp - \boldsymbol{b}\cdot\nabla\boldsymbol{U}\cdot\boldsymbol{b} + v_\parallel\nabla\cdot b\right)\frac{\partial f_{0s}}{\partial v_\perp}$$

$$+\left(-\boldsymbol{b}\cdot\frac{\mathrm{D}\boldsymbol{U}_\mathrm{E}}{\mathrm{D}t} + \frac{v_\perp^2}{2}\nabla\cdot\boldsymbol{b} + \frac{e}{m}E_\parallel\right)\frac{\partial f_{0s}}{\partial v_\parallel} = 0,$$

$$\sum_s e_s \int f_{0s}\,\mathrm{d}^3v = 0.$$

Introduction of kinetic pressures obtained from guiding center equation in (large-scale) anisotropic MHD

To summarize, the previous models still have the following problems:

- they do not take into account wave particle resonances at the origin of the dissipation of wave modes; in particular slow modes should be heavily damped.

- they lack a proper determination of FLR at small scales.

- the closure relations depend on the type of wave or the adiabatic/quasistatic regime

3D Vlasov-Maxwell simulations are hardly possible on present-day computers.

Gyrokinetic simulations (*G. Howes PoP **15**, 055904 , 2008)* are now feasible and show the presence of cascades both in the physical and velocity spaces in the range $k_\perp \rho \geq 1$.

Look for a model that can be integrated relatively fast, that allows for strong temperature anisotropies and that does not a priori order out the fast magnetosonic waves.

Fluid description retaining low-frequency kinetic effects: **Landau fluid models**

- Introduced by *Hammett & Perkins (PRL **64**, 3019, 1990)* as a closure retaining linear Landau damping.
- Applied to large-scale MHD by *Snyder, Hammett & Dorland (PoP **4**, 3974, 1997)* to close the hierarchy of moment equations derived from the drift kinetic equation.
- Extended to dispersive MHD with Hall effect and large scale FLR corrections *(Passot & Sulem, PoP **10**, 3906, 2003; Goswami, Passot & Sulem, PoP **12**, 102109, 2005)*
- Inclusion of quasi-transverse scales extending beyond the ion gyroscale, under the gyrokinetic scaling *(Passot & Sulem, PoP **14**, 082502, 2007)* : FLR-Landau fluids.

FLR-Landau fluids are based on a full description of the hydrodynamic nonlinearities, supplemented by a linear (or semi-linear) description of low-frequency kinetic effects (Landau damping and FLR corrections).

In contrast with gyrokinetics, Landau fluids retain fast waves that are accurately described away from resonances.

Note: I will not mention so-called FLR-MHD and many other fluid approaches!....

Alternative approach: gyrofluids

(Brizard 1992, Dorland & Hammett 1993, Beer & Hammett 1996)

- Obtained by taking velocity moments of the gyrokinetic equation.
- Nonlinear FLR corrections to all orders are captured.
- Linear closure of the hierarchy needed as for Landau fluids.
- All fast magnetosonic waves are ordered out: transverse velocity expressed in drift approximation.

Both Landau fluids and gyrofluid neglect wave particle trapping, i.e. the effect of particle bounce motion on the distribution function near resonance.

VII. The FLR-Landau fluid model

For the sake of simplicity, neglect electron inertia.

Ion dynamics: derived by computing velocity moments from Vlasov Maxwell equations.

$$\begin{cases} \partial_t \rho_p + \nabla \cdot (\rho_p u_p) = 0 \\ \partial_t u_p + u_p \cdot \nabla u_p + \dfrac{1}{\rho_p} \nabla \cdot \mathbf{p}_p - \dfrac{e}{m_p}(E + \dfrac{1}{c} u_p \times B) = 0 \\ E = -\dfrac{1}{c}\left(u_p - \dfrac{j}{ne}\right) \times B - \dfrac{1}{ne} \nabla \cdot \mathbf{p}_e, \\ \partial_t B = -c \nabla \times E \end{cases}$$

$$\rho_r = m_r n_r$$

quasi-neutrality $(n_e = n_p)$

$$j = \frac{c}{4\pi} \nabla \times B$$

pressure tensor $P_r = m_r n_r \int (v - u_r) \otimes (v - u_r) f_r d^3 v$
heat flux tensor $Q_r = m_r n_r \int (v - u_r) \otimes (v - u_r) \otimes (v - u_r) f_r d^3 v.$

$$\partial_t \mathbf{P}_r + u_r \cdot \nabla \mathbf{P}_r + \mathbf{P}_r \nabla \cdot u_r + \nabla \cdot \mathbf{Q}_r + [\mathbf{P}_r \cdot \nabla u_r + \frac{q_r}{m_r c} b \times \mathbf{P}_r]^{\mathcal{S}} = \mathbf{H}_r$$

zero in the absence of collisions

where the tensor $B \times \mathbf{p}_r$ has elements $(B \times \mathbf{p}_r)_{ij} = \epsilon_{iml} B_m p_{rlj}$

Although it could be advantageous to keep the fully nonlinear equation for the pressure tensor, leaving the modelization at the level of the heat flux tensor, it is easier at first to decompose the pressure as follows:

FLR corrections

$$\mathbf{p}_p = p_{\perp p}\mathbf{n} + p_{\parallel p}\boldsymbol{\tau} + \boldsymbol{\Pi}, \text{ with } \mathbf{n} = \mathbf{I} - \widehat{b} \otimes \widehat{b} \text{ and } \boldsymbol{\tau} = \widehat{b} \otimes \widehat{b}, \text{ where } \widehat{b} = B / |B|.$$

Electron pressure tensor is taken gyrotropic
(considered scales >> electron Larmor radius)
and thus characterized by the parallel and transverse pressures $p_{\parallel e}$ and $p_{\perp e}$.

Exact equations for the perpendicular and parallel pressures

heat flux tensor

$$\partial_t p_{\perp r} + \nabla\cdot(\vec{u}_r\, p_{\perp r}) + p_{\perp r}\nabla\cdot\vec{u}_r - p_{\perp r}\,\widehat{b}\cdot\nabla\vec{u}_r\cdot\widehat{b} + \frac{1}{2}\Big(\mathrm{tr}\,\nabla\cdot\mathbf{q}_r - \widehat{b}\cdot(\nabla\cdot\mathbf{q}_r)\cdot\widehat{b}\Big)$$
$$+\frac{1}{2}\Big(\mathrm{tr}\,(\boldsymbol{\Pi}\cdot\nabla\vec{u})^S - (\boldsymbol{\Pi}\cdot\nabla\vec{u})^S : \boldsymbol{\tau} + \boldsymbol{\Pi} : \frac{d\boldsymbol{\tau}}{dt}\Big)_r \delta_{rp} = 0$$

$$\partial_t p_{\parallel r} + \nabla\cdot(\vec{u}_r\, p_{\parallel r}) + 2p_{\parallel r}\,\widehat{b}\cdot\nabla\vec{u}_r\cdot\widehat{b} + \widehat{b}\cdot(\nabla\cdot\mathbf{q}_r)\cdot\widehat{b}$$
$$+\Big((\boldsymbol{\Pi}\cdot\nabla\vec{u})^S : \boldsymbol{\tau} - \boldsymbol{\Pi} : \frac{d\boldsymbol{\tau}}{dt}\Big)_r \delta_{rp} = 0,$$

work of the non-gyrotropic pressure force

Modelization of the heat flux tensor:

$\mathbf{q}_r = \mathbf{S}_r + \boldsymbol{\sigma}_r$ with $\boldsymbol{\sigma}_r : \mathbf{n} = 0$ and $\boldsymbol{\sigma}_r : \boldsymbol{\tau} = 0.$

The tensor S writes:

$$S_{ijk} = \tfrac{1}{2}(S_i^{\perp} n_{jk} + S_j^{\perp} n_{ik} + S_k^{\perp} n_{ij} + S_l^{\perp}\tau_{li} n_{jk} + S_l^{\perp}\tau_{lj} n_{ik} + S_l^{\perp}\tau_{lk} n_{ij})$$
$$+ S_i^{\parallel}\tau_{jk} + S_j^{\parallel}\tau_{ik} + S_k^{\parallel}\tau_{ij} - \tfrac{2}{3}(S_l^{\parallel}\tau_{li}\tau_{jk} + S_l^{\parallel}\tau_{lj}\tau_{ik} + S_l^{\parallel}\tau_{lk}\tau_{ij}),$$

The vectors $S^{//}$ and $S^{\perp}$ are defined by $\vec{S}_r^{\parallel} = \mathbf{q}_r : \boldsymbol{\tau}$ and $\vec{S}_r^{\perp} = \mathbf{q}_r : \mathbf{n}/2$

One has $q_{\perp r} = \vec{S}_r^{\perp} \cdot \widehat{b}$ and $q_{\parallel r} = \vec{S}_r^{\parallel} \cdot \widehat{b}.$

They are the only contributions to the gyrotropic heat flux tensor:

$$q_{r\ ijk}^{G} = q_{\parallel r}\hat{b}_i\hat{b}_j\hat{b}_k + q_{\perp r}(\delta_{ij}\hat{b}_k + \delta_{ik}\hat{b}_j + \delta_{jk}\hat{b}_i - 3\hat{b}_i\hat{b}_j\hat{b}_k).$$

One can write $\vec{S}_r^{\perp} = q_{\perp r}\widehat{b} + \vec{S}_{\perp r}^{\perp}$ and $\vec{S}_r^{\parallel} = q_{\parallel r}\widehat{b} + \vec{S}_{\perp r}^{\parallel}.$

The contribution of the tensor S in the pressure equations then reads:

$$\widehat{b}\cdot(\nabla\cdot\mathbf{S}_r)\cdot\widehat{b} = \nabla\cdot(q_{\parallel r}\widehat{b} + \vec{S}_{\perp r}^{\parallel}) - 2q_{\perp r}\nabla\cdot\widehat{b} - 2\widehat{b}\cdot\nabla\widehat{b}\cdot\vec{S}_r^{\parallel}$$

$$\frac{1}{2}\Big(\mathrm{tr}(\nabla\cdot\mathbf{S}_r) - \widehat{b}\cdot(\nabla\cdot\mathbf{S}_r)\cdot\widehat{b}\Big) = \nabla\cdot(q_{\perp r}\widehat{b} + \vec{S}_{\perp r}^{\perp}) + q_{\perp r}\nabla\cdot\widehat{b} + \widehat{b}\cdot\nabla\widehat{b}\cdot\vec{S}_r^{\parallel}$$

At the linear level, $\boldsymbol{\sigma}_r$ does not contribute to the heat flux terms in the equations for the gyrotropic pressures.

Nonlinear expressions of σ_r in the large-scale limit given in *Ramos, PoP* ***12****, 052102 (2005)*

Equations for the perpendicular and parallel gyrotropic heat fluxes

At this level some simplifications are introduced to reduce the level of complexity
(see Ramos 2005 for the full set of nonlinear equations)

Terms that involve the non-gyrotropic pressure and heat fluxes are kept only when they appear linearly

$$\partial_t q_{\parallel r} + \nabla\cdot(q_{\parallel r}\vec{u}_r) + 3q_{\parallel r}\hat{b}\cdot\nabla\vec{u}_r\cdot\hat{b} + 3p_{\parallel r}(\hat{b}\cdot\nabla)\left(\frac{p_{\parallel r}}{\rho}\right)$$
$$+\nabla\cdot(\widetilde{r}_{\parallel\parallel r}\hat{b}) - 3\widetilde{r}_{\parallel\perp r}\nabla\cdot\hat{b} + R^{NG}_{\parallel r} = 0$$

$$\partial_t q_{\perp r} + \nabla\cdot(\vec{u}_r q_{\perp r}) + q_{\perp r}\nabla\cdot\vec{u}_r + p_{\parallel} r(\hat{b}\cdot\nabla)\left(\frac{p_{\perp r}}{\rho}\right) + \delta_{rp}\frac{p_{\perp r}}{\rho}\left(\partial_x\Pi_{xz} + \partial_y\Pi_{yz}\right)_r$$
$$+\nabla\cdot(\widetilde{r}_{\parallel\perp r}\hat{b}) + \left((p_{\parallel r} - p_{\perp r})\frac{p_{\perp r}}{\rho} - \widetilde{r}_{\perp\perp r} + \widetilde{r}_{\parallel\perp r}\right)(\nabla\cdot\hat{b}) + R^{NG}_{\perp r} = 0,$$

Involve the 4th-rank gyrotropic cumulants: $\widetilde{r}_{\parallel\parallel}$, $\widetilde{r}_{\parallel\perp}$, $\widetilde{r}_{\perp\perp}$

$$\widetilde{r}_{\parallel\parallel} = r_{\parallel\parallel} - 3\frac{p_{\parallel}^2}{\rho},$$
$$\widetilde{r}_{\parallel\perp} = r_{\parallel\perp} - \frac{p_{\perp}p_{\parallel}}{\rho},$$
$$\widetilde{r}_{\perp\perp} = r_{\perp\perp} - 2\frac{p_{\perp}^2}{\rho}.$$

$R^{NG}_{\parallel}$ and $R^{NG}_{\perp}$ stand for the linear nongyrotropic contributions of the 4th-rank cumulants.

The completion of this model requires the determination of:

- closure relations to express the 4th-rank cumulants $\widetilde{r}_{\parallel\parallel}, \widetilde{r}_{\parallel\perp}, \widetilde{r}_{\perp\perp}$
  (closure at lower or higher order also possible)

  Only issue when dealing with the Large-Scale Landau fluid model (*Snyder, Hammett & Dorland, PoP* ***4****, 3974, 1997*).

- (non gyrotropic) FLR corrections to all moments.

Brief description of the hierarchy closure

The 4th-rank cumulants are obtained **from the linearized kinetic theory**,
assuming **small frequencies with respect to the ion gyrofrequency.**

(assuming long wavelengths with respect to the ion gyroradius or quasi-perpendicular directions).

IN PRACTICE:

*The kinetic expressions typically depend on electromagnetic field components and involve the plasma dispersion function (which is nonlocal both in space and **time**).*

These various expressions are expressed in terms of other fluid moments in such a way as to minimize the occurrence of the plasma dispersion function.

*The latter is otherwise replaced by suitable Padé approximants, thus leading to local-in-time expressions. At some places, a Hilbert transform with respect to the longitudinal space coordinate appears, that **modelizes Landau damping**.*

This procedure ensures consistency with the low-frequency linear kinetic theory, up to the use of Padé approximants.

Illustrate the basic idea on the electrostatic Vlasov model.

Linearized equation: $$(\partial_t + v\partial_x + (e/m)E\partial_v)f = 0$$

replace $$f = f^{(0)} + \epsilon f^{(1)}$$
$$\mathbf{B} = \mathbf{B}^{(0)} + \epsilon \mathbf{B}^{(1)}$$
$$\mathbf{E} = \epsilon \mathbf{E}^{(1)}$$

and get $$(\partial_t + v\partial_x) f^{(1)} = \frac{e\partial_x \phi}{m} \partial_v f^{(0)}.$$

leading to $$\boxed{f^{(1)} = k_x \frac{e\hat{\phi}}{m} \frac{\partial_v f^{(0)}}{(k_x v - \omega)}}$$

Linearized fluid moments:

$$\hat{n}^{(1)} = \int_{-\infty}^{+\infty} \mathrm{d}v f^{(1)}$$

$$\hat{u}^{(1)} = \frac{1}{n_0} \int_{-\infty}^{+\infty} \mathrm{d}v v f^{(1)}$$

$$\hat{p}^{(1)} = m \int_{-\infty}^{+\infty} \mathrm{d}v v^2 f^{(1)}$$

$$\hat{q}^{(1)} = m \int_{-\infty}^{+\infty} \mathrm{d}v v^3 f^{(1)} - 3 p_0 u^{(1)}$$

$$\hat{r}^{(1)} = m \int_{-\infty}^{+\infty} \mathrm{d}v v^4 f^{(1)}$$

Introducing the plasma function:

$$\sqrt{\pi}\mathrm{Z}(\mathrm{x}) \equiv \int_{-\infty}^{+\infty} \frac{\mathrm{e}^{-\mathrm{t}^2}}{\mathrm{t}-\mathrm{x}} \mathrm{dt} \quad \mathrm{Im}(\mathrm{x}) > 0$$

One gets:

$$\zeta = \frac{\omega}{|k_{\|}| v_{th}}$$

$$\hat{n}^{(1)} = -n_0 \frac{k_x}{|k_x|} \frac{e\hat{\phi}}{T_0} Z_1(\xi)$$

$$\hat{u}^{(1)} = -2^{1/2} v_{th} \frac{k_x}{|k_x|} \frac{e\hat{\phi}}{T_0} Z_2(\xi)$$

$$\hat{p}^{(1)} = -2 n_0 \frac{k_x}{|k_x|} e\hat{\phi} Z_3(\xi)$$

$$\frac{\hat{T}^{(1)}}{T_0} = \frac{p^{(1)}}{p^{(0)}} - \frac{n^{(1)}}{n_0}$$

$$\hat{q}^{(1)} = -3 P_0 u^{(1)} - n_0 e\hat{\phi} v_{th} \frac{k_x}{|k_x|} 2^{3/2} Z_4(\xi)$$

$$\hat{r}^{(1)} = -4 n_0 e\hat{\phi} \frac{k_x}{|k_x|} v_{th}^2 Z_5(\xi)$$

with the functions $Z_1(\zeta), \cdots, Z_5(\zeta)$ defined by the general formula:

$$Z_n(\zeta) = \frac{1}{2^n} \sum_{j=0}^{[n/2]} (-)^{n-2j} d_j(n) D^{(n-2j)} Z(\zeta)$$

One has:

$$Z_1(\xi) = R(\xi)$$

$$Z_2(\xi) = \xi R(\xi)$$

$$Z_3(\xi) = \frac{[1 + 2\xi^2 R(\xi)]}{2}$$

$$Z_4(\xi) = \frac{\xi[1 + 2\xi^2 R(\xi)]}{2}$$

$$Z_5(\xi) = \frac{3}{4} + \frac{\xi^2[1 + 2\xi^2 R(\xi)]}{2}.$$

and thus

$$\hat{n}^{(1)} = -n_0 \frac{k}{|k|} \frac{e\hat{\phi}}{T_0} R(\xi)$$

$$\hat{u}^{(1)} = -2^{1/2} v_{th} \frac{k}{|k|} \frac{e\hat{\phi}}{T_0} \xi R(\xi)$$

$$\hat{p}^{(1)} = -2 \frac{k}{|k|} e\hat{\phi} \frac{(1 + 2\xi^2 R(\xi))}{2} \; n_0$$

$$\hat{T}^{(1)} = -\frac{e\hat{\phi}}{T_0} \frac{k}{|k|} \left\{1 - R(\xi) + 2\xi^2 R(\xi)\right\} T_0$$

$$\hat{q}^{(1)} = 2^{1/2} n_0 e\hat{\phi} v_{th} \frac{k}{|k|} \xi (3R(\xi) - 2\xi^2 R(\xi) - 1)$$

Defining the cumulant:

$$\frac{\tilde{r}^{(1)}}{(p_0^2/\rho_0)} = \frac{\hat{r}^{(1)}}{(p_0^2/\rho_0)} - 6\frac{p_1}{p_0} + 3\frac{n_1}{n_0}$$

$$\tilde{r}^{(1)} = n_0 e\hat{\phi}\frac{k}{|k|}v_{th}^2(3 - 2\xi^2 - 3R(\xi) + 12\xi^2 R(\xi) - 4\xi^4 R(\xi)).$$

One also has:

$$\tilde{r}_{|||} = \sqrt{\frac{2T_{\|}^{(0)}}{m}}\frac{2\zeta^2[1+2\zeta^2R(\zeta)]+3[R(\zeta)-1]-12\zeta^2R(\zeta)}{2\zeta\,\mathrm{sgn}(k_z)[1-3R(\zeta)+2\zeta^2R(\zeta)]}\,q^{(1)}$$

$$\equiv \sqrt{\frac{2T_{\|}^{(0)}}{m}}\mathcal{F}_S q^{(1)}$$

and

$$\tilde{r}_{|||} = \frac{p_{\|}^{(0)}T_{\|}^{(0)}}{m}\frac{2\zeta^2[1+2\zeta^2R(\zeta)]+3[R(\zeta)-1]-12\zeta^2R(\zeta)}{1-R(\zeta)+2\zeta^2R(\zeta)}\frac{T_{\|}^{(1)}}{T_{\|}^{(0)}}$$

$$\equiv \frac{p_{\|}^{(0)}T_{\|}^{(0)}}{m}\mathcal{F}_T\frac{T_{\|}^{(1)}}{T_{\|}^{(0)}}.$$

Replace the response function by the following Padé approximant

$$R_4 = \frac{4 - 2i\sqrt{\pi}\zeta + (8 - 3\pi)\zeta^2}{4 - 6i\sqrt{\pi}\zeta + (16 - 9\pi)\zeta^2 + 4i\sqrt{\pi}\zeta^3(6\pi - 16)\zeta^4}$$

With this replacement, one has: $\lambda \frac{\mathcal{F}_S}{\mathcal{F}_T} + i\mu \frac{k_z}{|k_z|} = \mathcal{F}_S$

with $\lambda = (32-9\pi)/(3\pi-8)$ and $\mu = -2\sqrt{\pi}/(3\pi-8)$.

This leads to: $\tilde{r}_{|||} = \lambda p_{\parallel}^{(0)} \frac{T_{\parallel}^{(0)}}{m} \frac{T_{\parallel}^{(1)}}{T_{\parallel}^{(0)}} + \mu \sqrt{\frac{2T_{\parallel}^{(0)}}{m}} \frac{ik_z}{|k_z|}$. $q^{(1)}$

Landau damping is only appearing at the level of the closure relation, i.e. here in the fourth-order cumulant.

Diffusion of a temperature gradient

Comparaison between Vlasov and Landau fluid simulations

Vlasov (A. Mangeney and F. Califano)

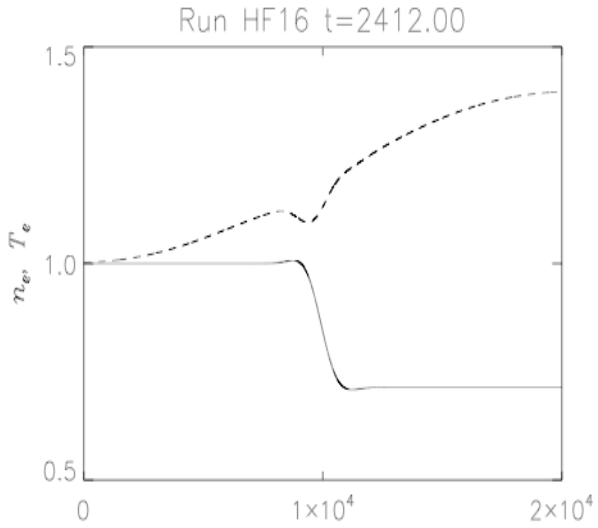

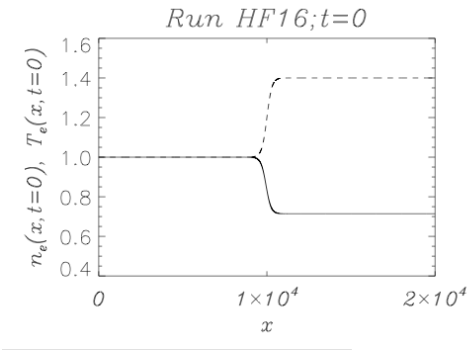

Initial condition

Domain size:
20 000 λ_e

Landau fluid

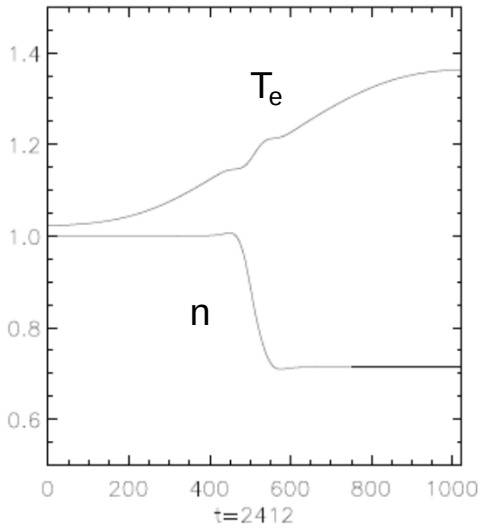

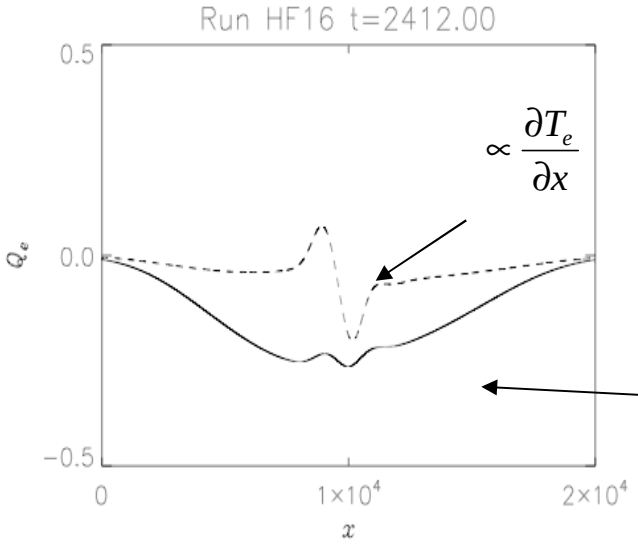

Parallel electron
heat flux

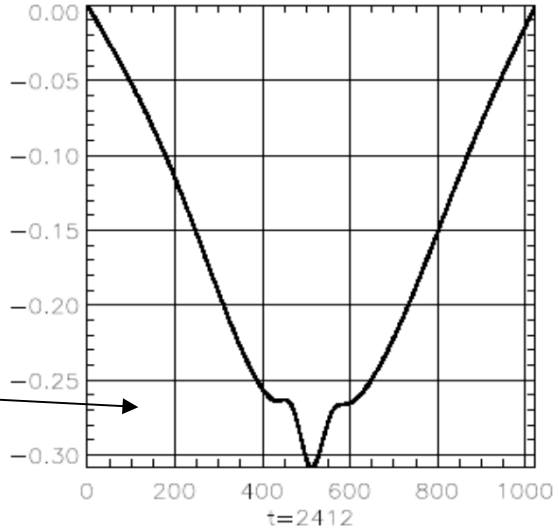

Hierarchy closure

from kinetic theory:

R: plasma response function

$$\zeta=(\omega/|k_z|)\sqrt{m/2T_{\parallel}^{(0)}}$$

$$b=T_{\perp}^{(0)}k_{\perp}^2/m\Omega^2=k_{\perp}^2 r_L^2/2$$

Larmor radius

$$\Gamma_\nu(b)=e^{-b}I_\nu(b)$$

Bessel modified function

At scales >> Larmor radius

$\Gamma_0(b)$ =1 $\Gamma_1(b)$ =0

For each species

$$\tilde{r}_{\parallel\parallel}=\frac{p_{\parallel}^{(0)}T_{\perp}^{(0)}}{m}\{2\zeta^2[1+2\zeta^2R(\zeta)]+3[R(\zeta)-1]-12\zeta^2R(\zeta)\}\times\left\{[\Gamma_1(b)-\Gamma_0(b)]\frac{b_z}{B_0}-\Gamma_0(b)\frac{e\Psi}{T_{\perp}^{(0)}}\right\}$$

$$\tilde{r}_{\parallel\perp}=\frac{p_{\perp}^{(0)2}}{\rho^{(0)}}[1-R(\zeta)+2\zeta^2R(\zeta)]\left\{[2b\Gamma_0(b)-\Gamma_0(b)-2b\Gamma_1(b)]\frac{b_z}{B_0}+b[\Gamma_0(b)-\Gamma_1(b)]\frac{e\Psi}{T_{\perp}^{(0)}}\right\}$$

These formulas can be expressed in terms of lower order fluid moments.

Using 4-pole Padé:

$$R_4(\zeta)=\frac{4-2i\sqrt{\pi}\zeta+(8-3\pi)\zeta^2}{4-6i\sqrt{\pi}\zeta+(16-9\pi)\zeta^2+4i\sqrt{\pi}\zeta^3+(6\pi-16)\zeta^4},$$

one gets:

$$\tilde{r}_{\parallel\parallel r}=\frac{32-9\pi}{2(3\pi-8)}n_0v_{\mathrm{th}\parallel r}^2T'_{\parallel r}-\frac{2\sqrt{\pi}}{3\pi-8}v_{\mathrm{th}\parallel r}\frac{ik_z}{|k_z|}q_{\parallel r}$$

In physical space: negative Hilbert transform: signature of Landau resonance

overline: *instantaneous space average*
prime: *fluctuations*

Using 2-pole Padé:

$$R_2(\zeta)=1/(1-i\sqrt{\pi}\zeta-2\zeta^2)$$

one gets:

$$\tilde{r}_{\parallel\perp p}=-\frac{\sqrt{\pi}}{2}v_{\mathrm{th}\parallel p}\frac{ik_z}{|k_z|}\left[q_{\perp p}+\frac{1}{\Omega_p}(\Gamma_0(b)-\Gamma_1(b))\frac{\overline{p}_{\perp p}}{\rho_0}(\overline{p}_{\perp p}-\overline{p}_{\parallel p})(i\vec{k}_\perp\times\frac{\vec{b}_\perp}{B_0})_z\right]$$

$$\tilde{r}_{\parallel\perp e}=-\frac{\sqrt{\pi}}{2}v_{\mathrm{th}\parallel e}\frac{ik_z}{|k_z|}\left[q_{\perp e}-\frac{1}{\Omega_p}\frac{\overline{p}_{\perp e}}{\rho_0}(\overline{p}_{\perp e}-\overline{p}_{\parallel e})(i\vec{k}_\perp\times\frac{\vec{b}_\perp}{B_0})_z\right]$$

at large scales $\tilde{r}_{\perp\perp}=0$

At which level is it appropriate to close the hierarchy?

Keeping higher fluid moments allows one to account for distortions of the distribution function and to keep more fluid nonlinearities.

Taking a higher order Padé approximant leads to more precise approximations. But, except in particular cases, all the ζ terms cannot be eliminated, thus leading to closure relations in the form of linear PDEs instead of algebraic relations.

This is thus analogous to closing the fluid hierarchy at a higher moment, possibly with a Padé of lower order.

Example:
Take R_3 instead of R_2 for $\tilde{r}_{\parallel\perp}$ leads to:

$$\left(\frac{d}{dt}-2|a_0|\sqrt{\frac{2T_\parallel^{(0)}}{m}}\mathcal{H}_z\partial_z\right)\tilde{r}_{\parallel\perp}+\frac{2T_\parallel^{(0)}}{m}\left(a_1-\frac{1}{2}\right)$$
$$\times\partial_z\left[q_\perp+[\Gamma_0(b)-\Gamma_1(b)]\frac{p_\perp^{(0)}}{v_A^2}\left(\frac{T_\perp^{(0)}-T_\parallel^{(0)}}{m_p}\right)\frac{j_z}{en^{(0)}}\right]=0.$$

Problem: preserving Galilean invariance introduces one nonlinear term. Many others are missing!

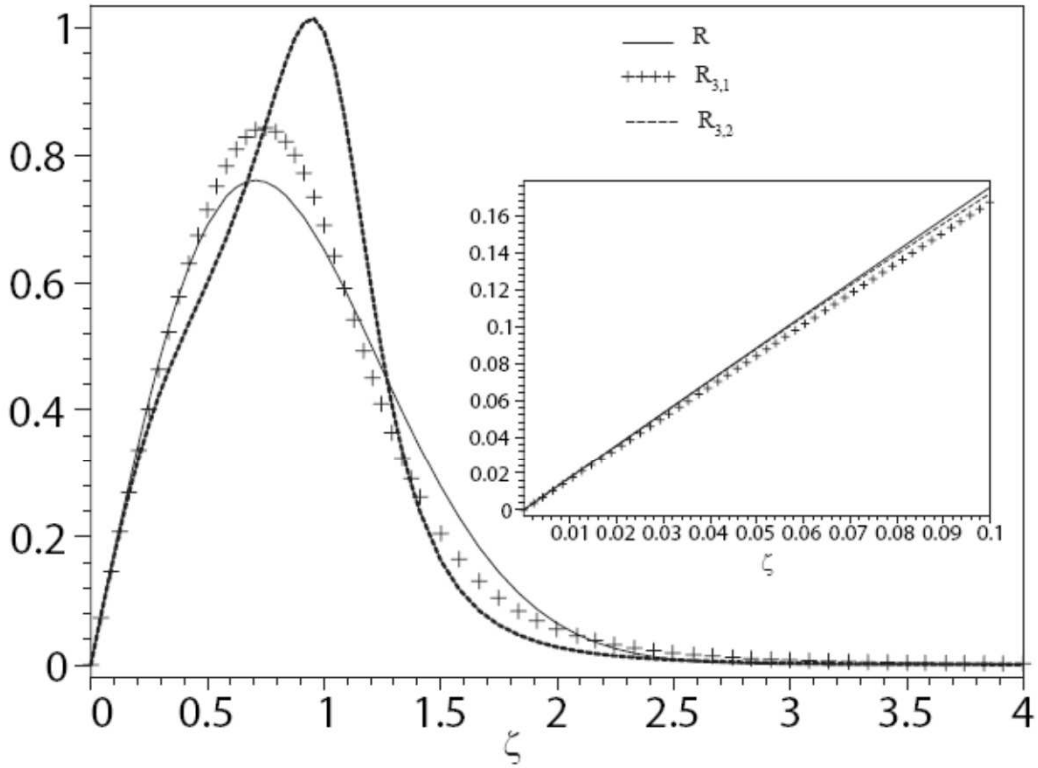

FIG. 1: Comparison between the imaginary part of the function $R(\zeta)$ (thin solid line) with the corresponding Padé approximants $R_{3,1}$ (crosses) and $R_{3,2}$ (thick dashed line). The insert displays the same quantities in a smaller range of ζ, close to the origin.

Several choices of Padé approximant are possible. We choose one that has a globally better fit, even if another one performs slighlty better at large scales

When restricting to large scales, thus neglecting the Hall and FLR terms, this system develops microinstabilities that lead to blow up.

Assuming that the state of the plasma remains limited by the marginal stability limit, a heuristic method was used in Sharma et al. (ApJ **637**, 952 (2006)) in the context of MRI in accretion disks.

Introduction of collisions in this type of closures is possible:

See: Sharma & Hammett, ApJ **596**, 1121 (2003)
Chang & Callen Phys. Fluids B **4,** 1167 (1992) and **4,** 1182 (1992)

Using the (too simple) form of BGK collision operator

$$\partial_t f_s + \mathbf{v}\cdot\nabla f_s + \frac{q_s}{m_s}\left(\mathbf{E} + \frac{\mathbf{v}}{c}\times\mathbf{B}\right)\cdot\nabla f_s = C(f_s)$$

$$C(f_j) = -\sum_k \nu_{jk}(f_j - F_{Mjk}) \quad \text{with,}$$

$$F_{Mkj} = \frac{n_k}{\pi^{3/2} v_{th,k}^3} e^{-\frac{(v_z-u_{z,j})^2}{v_{th,k}^2}} e^{-\frac{(v_y-u_{y,j})^2}{v_{th,k}^2}} e^{-\frac{(v_x-u_{x,j})^2}{v_{th,k}^2}}$$

$$V_{th,k} = \left(\frac{2T_k}{m_k}\right)^{1/2} \qquad \nu_{ii} = \nu_{ee}\left(\frac{m_e}{m_i}\right)^{\frac{1}{2}}$$

$$T_k = \left(\frac{T_\parallel + 2T_\perp}{3}\right) \qquad \nu_{ie} = \nu_{ee}\left(\frac{m_e}{m_i}\right)$$

$$\nu_s = \nu_{ii} + \nu_{ie}$$

Gross &Krook, Phys. Rev. **102**, 593 (1956).
Bhatnagar, Z. Astrophys. **54**, 234 (1962).
Green, Phys. Fluids **11**, 2022 (1973).
Livi & Marsh, Phys. Rev. A **34**, 533 (1986).

leads to additional terms :

in the r.h.s. of pressure equation

$$C_{\perp r} = \frac{1}{3}(\nu_{rr} + \nu_{r\overline{r}})\frac{\rho}{\rho_0}(p_{\parallel r} - p_{\perp r}) + \frac{1}{2}\frac{m_i \nu_{ie}}{n_0 e^2}[j^2 - (j \cdot \widehat{b})^2] \tag{8}$$

$$C_{\parallel r} = -\frac{2}{3}(\nu_{rr} + \nu_{r\overline{r}})\frac{\rho}{\rho_0}(p_{\parallel r} - p_{\perp r}) + \frac{m_i \nu_{ie}}{n_0 e^2}(j \cdot \widehat{b})^2 \tag{9}$$

in the r.h.s. of heat flux equation

$$Q_{\parallel r} = -(\nu_{rr} + \nu_{r\overline{r}})\frac{\rho}{\rho_0} q_{\parallel r} \mp \nu_{r\overline{r}}(p_{\parallel r} + 2p_{\perp r})\frac{j \cdot \widehat{b}}{e n_0} \mp \nu_{ie}\frac{m_i^2}{e^3 n_0}\frac{1}{\rho}(j \cdot \widehat{b})^3 \tag{10}$$

$$Q_{\perp r} = -(\nu_{rr} + \nu_{r\overline{r}})\frac{\rho}{\rho_0} q_{\perp r} \mp \frac{1}{3}\nu_{r\overline{r}}(p_{\parallel r} + 2p_{\perp r})\frac{j \cdot \widehat{b}}{e n_0} \mp \frac{1}{2}\nu_{ie}\frac{m_i^2}{e^3 n_0}\frac{1}{\rho}[j^2 - (j \cdot \widehat{b})^2](j \cdot \widehat{b}). \tag{11}$$

with, in addition, the Joule term in the magnetic field equation (allowing for energy conservation) and a linear term in the fourth order cumulant equation $r_{//\perp}$

Sulem and Passot, AIP Conf. Proc. **1439**, 99 (2012).

Two methods to determine the non-gyrotropic elements of the tensors

I. Solve the (coupled) algebraic equations that result from the projection the tensorial pressure equations, orthogonally to the gyrotropic "directions".

At the level of the pressure:

$\Pi_r \longrightarrow \mathbf{P}_r \times \widehat{b} - \widehat{b} \times \mathbf{P}_r = \mathbf{k}_r$

$$\mathbf{k}_r = \frac{1}{\Omega_r}\frac{B_0}{|b|}[\frac{d\mathbf{P}_r}{dt} + (\nabla \cdot u_r)\mathbf{P}_r + \nabla \cdot \mathbf{Q}_r + (\mathbf{P}_r \cdot \nabla u_r)^{\mathcal{S}}].$$

The left hand side $\mathbf{P}_r \times \widehat{b} - \widehat{b} \times \mathbf{P}_r$ can be viewed as a self-adjoint linear operator acting on $\mathbf{P}_r$, whose kernel is spanned by the tensors $(\mathbf{I} - \widehat{b} \otimes \widehat{b})$ and $\widehat{b} \otimes \widehat{b}$.

The solvability conditions lead to the dynamical equations for pressures and heat fluxes

Exact solution for the gyroviscous tensor:

$$\Pi_r = \frac{1}{4}[\widehat{b} \times \overline{\mathbf{k}}_r \cdot (\mathbf{I} + 3\widehat{b} \otimes \widehat{b})]^{\mathcal{S}}$$

Projection on the image:

$$\overline{\mathbf{a}} = \mathbf{a} - \frac{1}{2}\mathbf{a} : (\mathbf{I} - \widehat{b} \otimes \widehat{b})(\mathbf{I} - \widehat{b} \otimes \widehat{b}) - (\mathbf{a} : \widehat{b} \otimes \widehat{b})\widehat{b} \otimes \widehat{b},$$

Since Π also appears in the r.h.s., this procedure requires an expansion in a small parameter, usually taken as the time and space scale separation with the ion gyroscales.

Leads to the **Meso-Scale Landau fluid model**.

This formula has the great advantage of being fully nonlinear.
Its algebraic complexity, however precludes an easy numerical implementation.

A second order solution of coupled equations for the vectors S and the tensor Π is possible and was explicited in a linear setting in *Goswami, Passot & Sulem, PoP **12**, 102109 (2005).*

The resulting model is refined in *Passot, Sulem & Hunana, PoP **19**, 082113 (2012)*
by retaining two additional ingredients:

- Full description of the heat flux tensor
  (tensor **σ** taken from Ramos PoP **12**, 052102 ,2005)
- Non-gyrotropic contributions R_{NG} of the fourth-rank tensor
  (entering the equation for $q_{//}$ and $q_{\perp}$).

These additions are required in order to reproduce the linear growth rate of the mirror instability, and in particular the restabilization at small scales.

Mirror-instability threshold captured by LS Landau fluids (including only Landau damping).

$$\begin{cases} \Pi_{xx}^{(1)} = -\dfrac{\overline{p}_{\perp p}}{2\Omega_p}(\partial_x u_y + \partial_y u_x), \\ \Pi_{xy}^{(1)} = \dfrac{\overline{p}_{\perp p}}{2\Omega_p}(\partial_x u_x - \partial_y u_y), \end{cases}$$

σ contributes to the gyroviscosity at a linear level.

$$\begin{cases} \Pi_{xx}^{(2)} = -\dfrac{1}{2\Omega_p}[\partial_t \Pi_{xy}^{(1)} + \dfrac{1}{2}(\partial_x S_y^{\perp(1)} + \partial_y S_x^{\perp(1)}) + (\nabla\cdot\sigma)_{12}], \\ \Pi_{xy}^{(2)} = \dfrac{1}{2\Omega_p}[\partial_t \Pi_{xx}^{(1)} + \dfrac{1}{2}(\partial_x S_x^{\perp(1)} - \partial_y S_y^{\perp(1)}) + (\nabla\cdot\sigma)_{11}], \end{cases}$$

$$\vec{\Pi}_z^{(1)} = \frac{1}{\Omega_p}\hat{z}\times[\overline{p}_{\parallel p}\partial_z \vec{u}_\perp + \overline{p}_{\perp p}\nabla_\perp u_z - (\overline{p}_{\perp p} - \overline{p}_{\parallel p})\partial_t \hat{b} + \nabla_\perp q_{\perp p}],$$

$$\vec{\Pi}_z^{(2)} = \frac{1}{\Omega_p}\hat{z}\times(\partial_t \vec{\Pi}_z^{(1)} + \partial_z S_\perp^{\parallel(1)} + \vec{\partial}\sigma_3)$$

$$\Pi_{yy} = -\Pi_{xx}$$

$$\Pi_{zz} = 0,$$

$$\begin{cases} S_\perp^{\perp(1)} = \dfrac{2}{\Omega_p}\dfrac{\overline{p}_{\perp p}}{m_p}\hat{z}\times\nabla_\perp T'_\perp \\ S_\perp^{\parallel(1)} = \dfrac{1}{\Omega_p}\hat{z}\times[\dfrac{\overline{p}_{\perp p}}{m_p}\nabla_\perp T'_\parallel + 2\Big(\dfrac{\overline{p}_{\parallel p} - \overline{p}_{\perp p}}{m_p}\Big)\overline{T}_\parallel \partial_z \hat{b}_\perp + \nabla_\perp \tilde{r}_{\parallel\perp}], \end{cases}$$

$$\begin{cases} S_\perp^{\perp(2)} = \dfrac{1}{\Omega_p}\hat{z}\times(\partial_t S_\perp^{\perp(1)} + \dfrac{\overline{T}_\perp}{m_p}\nabla_\perp\cdot\Pi_\perp^{(1)}) \\ S_\perp^{\parallel(2)} = \dfrac{1}{\Omega_p}\hat{z}\times(\partial_t S_\perp^{\parallel(1)} + \dfrac{2\overline{T}_\parallel}{m_p}\partial_z \vec{\Pi}_z^{(1)}), \end{cases}$$

where

$$\boldsymbol{\sigma}_r = \frac{\overline{p}_{\perp r}(\overline{p}_{\parallel r} - \overline{p}_{\perp r})}{4eB_0 n}\mathbf{a}^S$$

$$a_{\alpha\beta\gamma} = \epsilon_{\alpha\lambda\mu}\tau_{\beta\lambda}n_{\gamma\nu}\Big(\partial_\nu \hat{b}_\mu + \partial_\mu \hat{b}_\nu\Big)$$

$$(\vec{\partial}\sigma)_3 = ((\nabla\cdot\sigma)_{13}, ((\nabla\cdot\sigma)_{23}).$$

One has:

$$(\nabla\cdot\sigma)_{11} = -2\alpha\partial_z(\partial_x \hat{b}_y + \partial_y \hat{b}_x),$$

$$(\nabla\cdot\sigma)_{12} = 2\alpha\partial_z(\partial_x \hat{b}_x - \partial_y \hat{b}_y),$$

$$(\nabla\cdot\sigma)_{13} = -2\alpha\Delta_\perp \hat{b}_y,$$

$$(\nabla\cdot\sigma)_{23} = 2\alpha\Delta_\perp \hat{b}_x,$$

$$\alpha = \frac{c}{4eB_0}\frac{\overline{p}_{\perp p}(\overline{p}_{\parallel p} - \overline{p}_{\perp p})}{n_0}.$$

$$(\nabla\cdot\sigma)_{22} = -(\nabla\cdot\sigma)_{11}$$

$$(\nabla\cdot\sigma)_{33} = 0$$

- **Second order terms** are required to capture the **dispersion relation of KAWs** and **magnetosonic waves**

*Hazegawa & Chen, Phys. Fluids, **19**, 1924 (1976)*

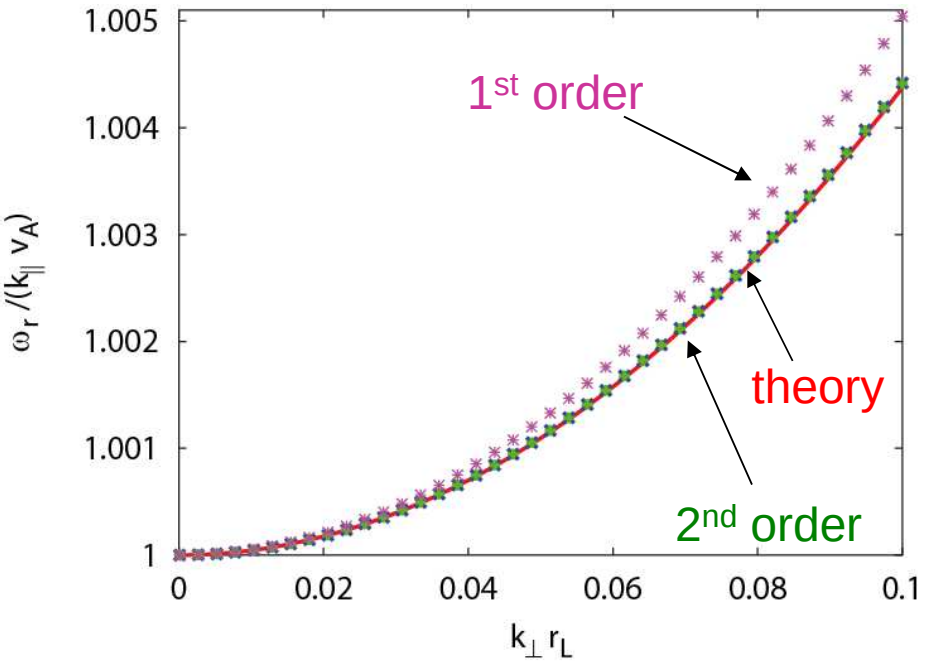

KAW, β=0.01, τ=1, θ =atan(1000)

Theory:

$$\tau = T_{\parallel e}/T_{\parallel p}$$

$$\frac{\omega}{k v_A \cos\theta} = 1 + \frac{1}{2}\frac{T_e}{T_p}\left(1 + \frac{3T_p}{4T_e}\right)\frac{T_p}{m\Omega_p^2}k_\perp^2$$

valid when $\frac{m_e}{m_p} \ll \beta \ll \frac{T_e}{T_p}$ where $\beta = \frac{1}{v_A^2}\frac{T_e}{m_p}$

*Mikhailovskii & Smolyakov, JETP **61**, 109 (1985)*

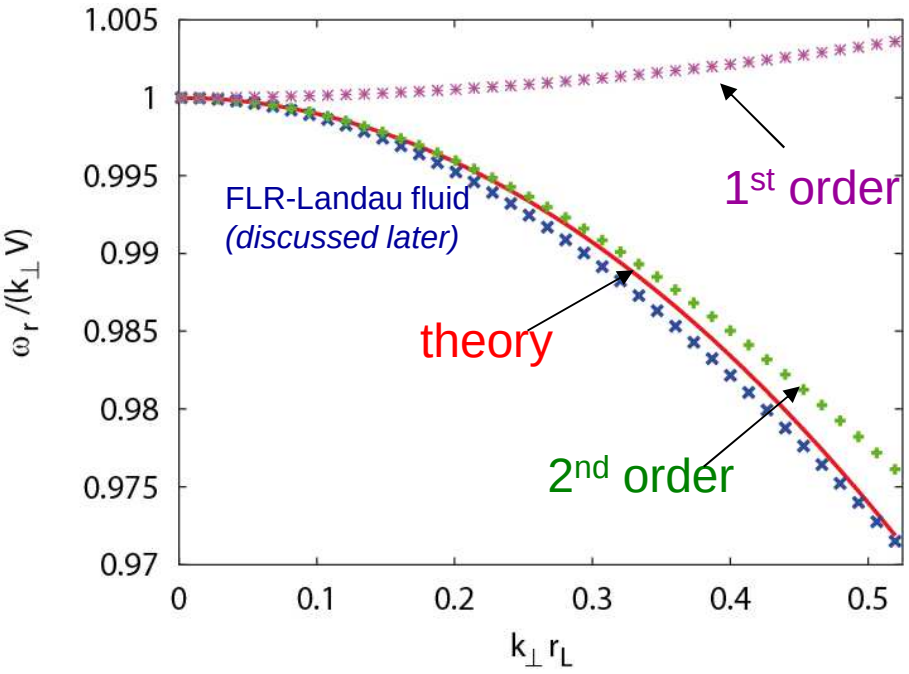

Magnetosonic waves: β=3, τ=1, θ=π/2

Theory:

$$\omega^2 = k^2 V^2 (1 - k^2 a_D^2)$$

$$V^2 = c_A^2 (1 + \beta)$$

$$a_D^2 = \frac{\rho^2}{4}\frac{1 + \beta_e + 5/2\beta_i}{1+\beta}$$

ρ≡r_L

Mirror growth rate:

In the case of cold electrons an analytic derivation of the growth rate was performed.

this leads to:

$$\partial_t\left(\frac{b_z}{B_0}\right) = \sqrt{\frac{2}{\pi}}\sqrt{\frac{T_\parallel^{(0)}}{m}}\frac{T_\parallel^{(0)}}{T_\perp^{(0)}}(-\mathcal{H}\partial_z)\Big[\Big(\frac{T_\perp^{(0)}}{T_\parallel^{(0)}} - 1 - \frac{1}{\beta_\perp}\Big)\frac{b_z}{B_0}$$

$$-\frac{1}{\beta_\perp}\Big(1+\frac{\beta_\perp-\beta_\parallel}{2}\Big)\Delta_\perp^{-1}\partial_{zz}\frac{b_z}{B_0} + \Big(\frac{1}{\beta_\perp}\Big(3-\frac{3}{2}-\alpha\Big)\frac{T_\perp^{(0)}}{m\Omega^2}\Delta_\perp\frac{b_z}{B_0}\Big],$$

(see Sulem's lecture)

contribution from R_{NG} $\quad \frac{1}{p_\perp^{(0)}}\nabla_\perp\cdot\boldsymbol{\Pi}_\perp$ $\quad \nabla_\perp\cdot\Pi_{\perp z}$

The last term is equal to -3/2 if evaluated from kinetic theory;
in the fluid framework its correct determination needs to take into account the heat flux contribution σ.

With these ingredients, the growth rate identifies with that of the kinetic theory.

Note that a fluid closure that neglects R_{NG} leads to an ill-posed problem.

This Meso-Scale Landau fluid model, nevertheless leads to spurious instability *(beyond its range of validity)* for KAWs when temperature anisotropy is too large.

$\beta_{||}=1.5$

$a_p=1.495$

$\tau=1.0$

$a_e=1.0$

$\theta= 85°$

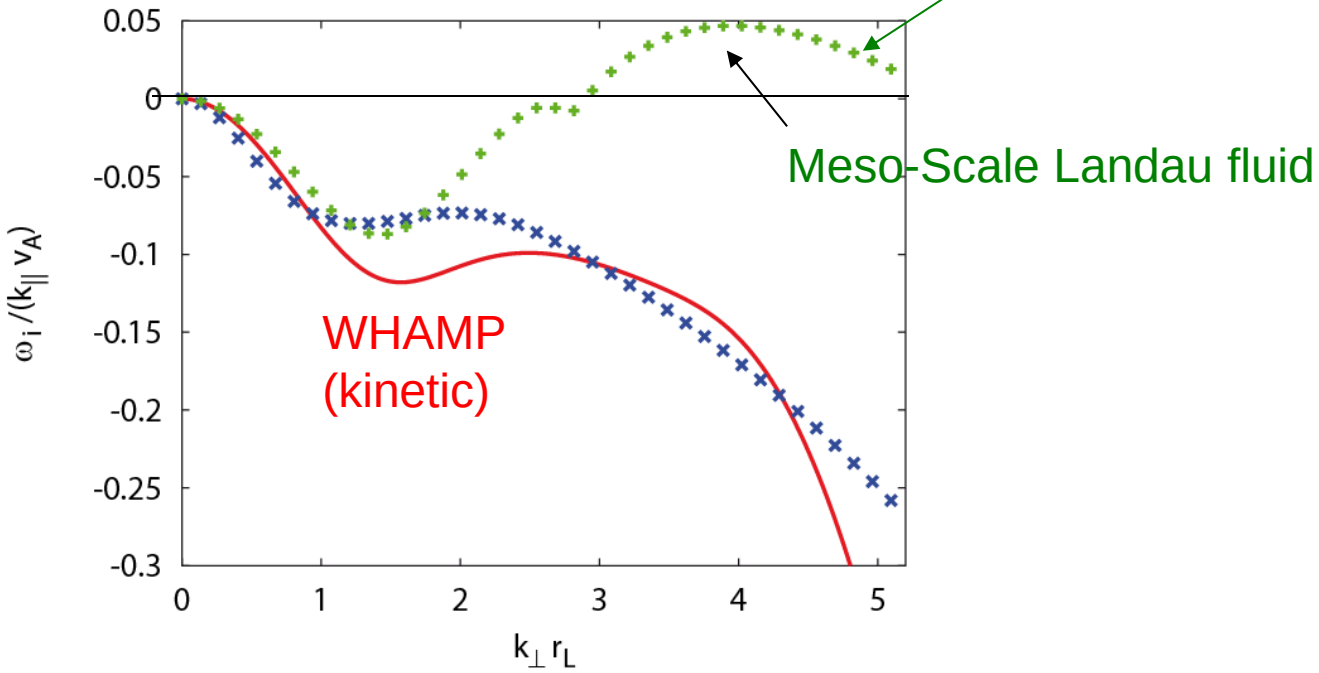

Although the instability occurs beyond the spectral validity range of the model, such unstable scales are usually present in simulations not limited to the largest MHD scales.

In such a regime, an accurate description of the small scales is required, at least at a linear level.

II. The other possiblity to determine FLR contributions is to use the linear kinetic theory in the low-frequency limit: $\omega/\Omega \sim \epsilon \ll 1$
(for a bi-Maxwellian d.f.)

In this case, the expansion is valid for:

- quasi-transverse fluctuations $(k_\parallel/k_\perp \sim \epsilon)$ with $k_\perp r_L \sim 1$
- hydrodynamic scales with $k_\parallel r_L \sim k_\perp r_L \sim \epsilon.$ r_L : ion Larmor radius

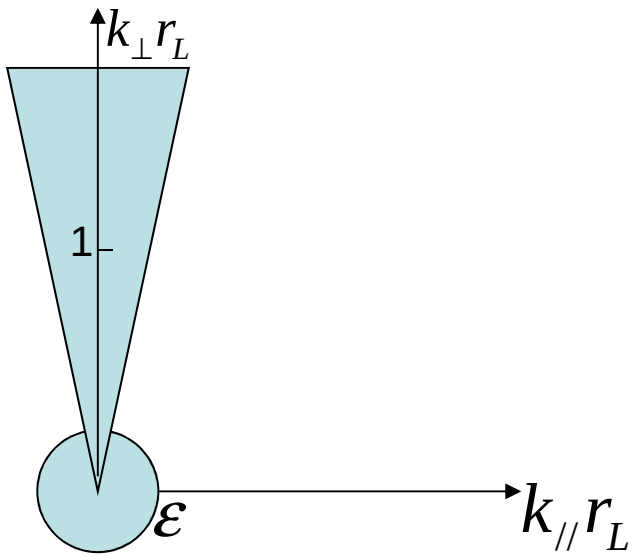

$$r_L^2 = \frac{v_{th_\perp}^2}{\Omega^2} = \frac{2T_\perp}{m_i \Omega^2}$$

All fluid moments are calculated **from the linearized kinetic theory**, *assuming* small frequencies with respect to the ion gyrofrequency.

This step involves exactly the same assumptions as **gyrokinetics**:

IN FACT: the dispersion relation of the plasma modes, obtained from the quasi-neutrality equations together with parallel and perpendicular Ampere's laws after plugging the ion and electron densities and velocities calculated from this low-frequency kinetic theory, is identical to the gyrokinetic one (Howes et al. ApJ 651:590–614 (2006)).

Since it includes temperature anisotropy, it allows one to derive the mirror instability growth rate with hot electrons in its full generality (Kuznetsov et al. PoP 19, 090701 (2012))

FLR terms:

$$\Pi_{xx} = -\Pi_{yy} = \overline{p}_{\perp p}\Big(- \frac{k_x^2 - k_y^2}{k_\perp^2}\mathcal{A} + 2\frac{k_x k_y}{k_\perp^2}\mathcal{B}\Big)$$

$$\Pi_{yx} = \Pi_{xy} = \overline{p}_{\perp p}\Big(- 2\frac{k_x k_y}{k_\perp^2}\mathcal{A} - \frac{k_x^2 - k_y^2}{k_\perp^2}\mathcal{B}\Big)$$

$$\Pi_{xz} = \Pi_{zx} = -ik_x\mathcal{C} + ik_y\mathcal{D}$$

$$\Pi_{yz} = \Pi_{zy} = -ik_y\mathcal{C} - ik_x\mathcal{D}$$

$$\Pi_{zz} = 0,$$

$$\vec{S}^{\perp}_{\perp r} = -\nabla_\perp \mathcal{E}_r + \nabla_\perp \times (\mathcal{F}_r \widehat{z})$$

$$\vec{S}^{\parallel}_{\perp r} = -\nabla_\perp \mathcal{G}_r + \nabla_\perp \times (\mathcal{H}_r \widehat{z}).$$

with

instantaneous space averages

$$\mathcal{E}_p = \frac{-\overline{p}_{\perp p}}{k_\perp^2}\Big\{\mathfrak{E}_1(b)\frac{c}{B_0}(i\vec{k}_\perp \times \vec{E}_\perp)_z - \mathfrak{E}_3(b)(i\vec{k}_\perp \cdot \vec{u}_{\perp p})\Big\}.$$

functions of transverse wavenumbers involving modified Bessel functions

$$\mathcal{A} = \frac{1}{\Omega_p}\mathfrak{A}_1(b)(i\vec{k}_\perp \times \vec{u}_{\perp p})_z + \mathfrak{A}_2(b)\frac{T'_{\perp p}}{\overline{T}_{\perp p}}$$

$$\mathcal{B} = -\frac{c}{\Omega_p B_0}\mathfrak{B}_1(b)(i\vec{k}_\perp \times \vec{E}_\perp)_z + \frac{1}{\Omega_p}\mathfrak{B}_2(b)(i\vec{k}_\perp \cdot \vec{u}_{\perp p}).$$

$$\mathcal{C} = \overline{p}_{\parallel p}\Big[- \Big(\frac{\overline{T}_{\perp p}}{\overline{T}_{\parallel p}} - 1\Big)\mathfrak{C}_1(b)\frac{1}{k_\perp^2}\Big(i\vec{k}_\perp \cdot \frac{\vec{b}_\perp}{B_0}\Big)$$

$$+\frac{c}{\Omega_p B_0}\mathfrak{C}_2(b)\Big(E_z - \Big(\frac{\overline{T}_{\perp p}}{\overline{T}_{\parallel p}} - 2\Big)\frac{ik_z}{k_\perp^2}(i\vec{k}_\perp \cdot \vec{E}_\perp)\Big)\Big].$$

$$\mathcal{G}_p = \frac{2}{\Omega_p}\frac{\overline{T}_{\parallel p}}{m_p}(\overline{p}_{\perp p} - \overline{p}_{\parallel p})\mathfrak{C}_2(b)\frac{1}{k_\perp^2 B_0}ik_z(i\vec{k}_\perp \times \vec{b}_\perp)_z$$

$$\mathcal{G}_e = -\frac{2}{\Omega_p}\frac{\overline{T}_{\parallel e}}{m_p}(\overline{p}_{\perp e} - \overline{p}_{\parallel e})\frac{1}{k_\perp^2 B_0}ik_z(i\vec{k}_\perp \times \vec{b}_\perp)_z.$$

also relevant for electrons

A more sophisticated treatment is necessary for the *D* term:
perpendicular pressure balance is to be imposed and $q_\perp$ has to be obtained form T

- The model conserves the total energy:

$$E = \int \left[\frac{\rho |u|^2}{2} + \frac{|b|^2}{2} + \beta_{\|i} \left(p_{\perp i} + p_{\perp e} + \frac{1}{2}(p_{\|i} + p_{\|e}) \right) \right] d\mathbf{x}$$

  Conservation of energy is independent of the heat fluxes and subsequent equations, but requires retaining the work done by the FLR stress forces.

- Implementation of the Landau damping via Hilbert transforms, and also of the FLR coefficients as Bessel functions of $k_\perp \rho$, is easy in a spectral code.

- Electron Landau damping is an essential ingredient in many cases (limiting the range of validity of isothermal electrons often used in hybrid simulations).

- All linearized fluid equations are satisfied when plugging the fluid moments directly calculated from the LF kinetic theory, except the perpendicular velocity equation: it reduces to the perpendicular pressure balance condition, as in gyrokinetics.

Dispersion relation of low frequency modes: comparison with linear kinetic theory

Mirror modes:

Normalized growth rate ω_i/Ω_p versus $k_\perp r_L$

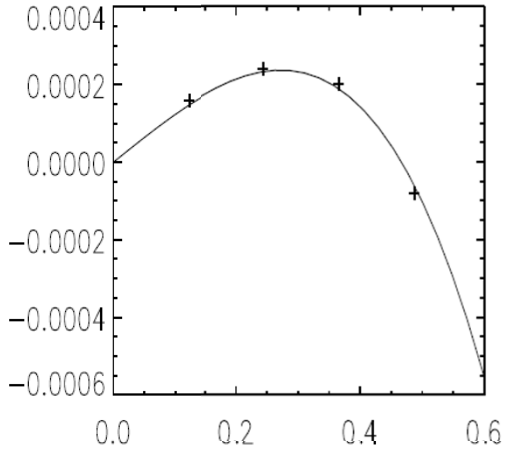

$\tau = T_{\|e}/T_{\|p}$

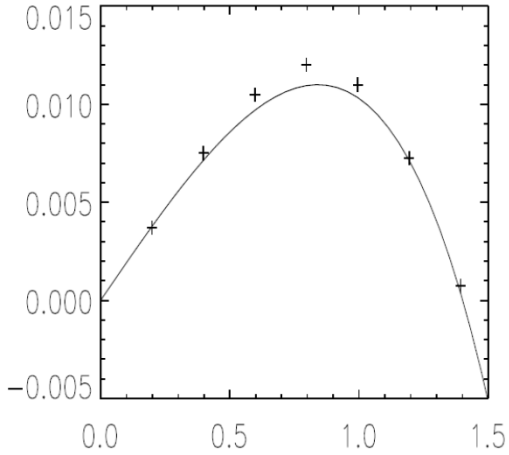

$\beta = 5,\ \tau = 0.1,\ \theta = \cos^{-1}(.1),$
$T_{\perp p}/T_{\|p} = 1.2$ and $T_{\perp e}/T_{\|e} = 1.$

$\beta = 2,\ \tau = 1,\ \theta = \cos^{-1}(.1),$
$T_{\perp p}/T_{\|p} = 2$ and $T_{\perp e}/T_{\|e} = 1.$

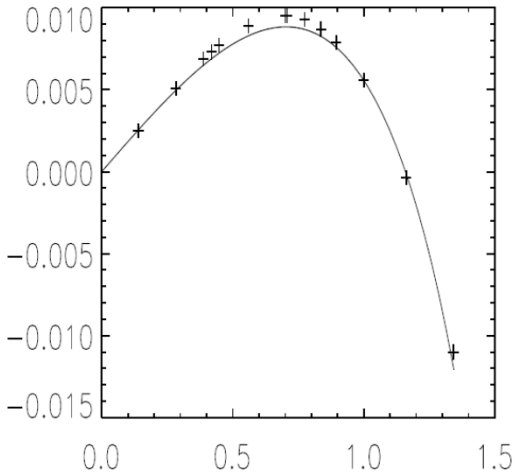

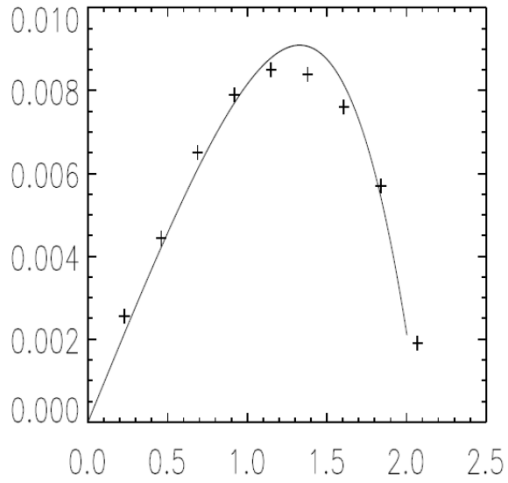

$\beta = 5,\ \tau = 1,\ \theta = \cos^{-1}(.2),$

$T_{\perp p}/T_{\|p} = 1.4$ and $T_{\perp e}/T_{\|e} = 1.$

$T_{\perp p}/T_{\|p} = 1.1$ and $T_{\perp e}/T_{\|e} = 1.18$

Frequency and damping rate of Alfvén waves:

quasi-transverse propagation (Kinetic Alfvén waves)

frequency damping rate

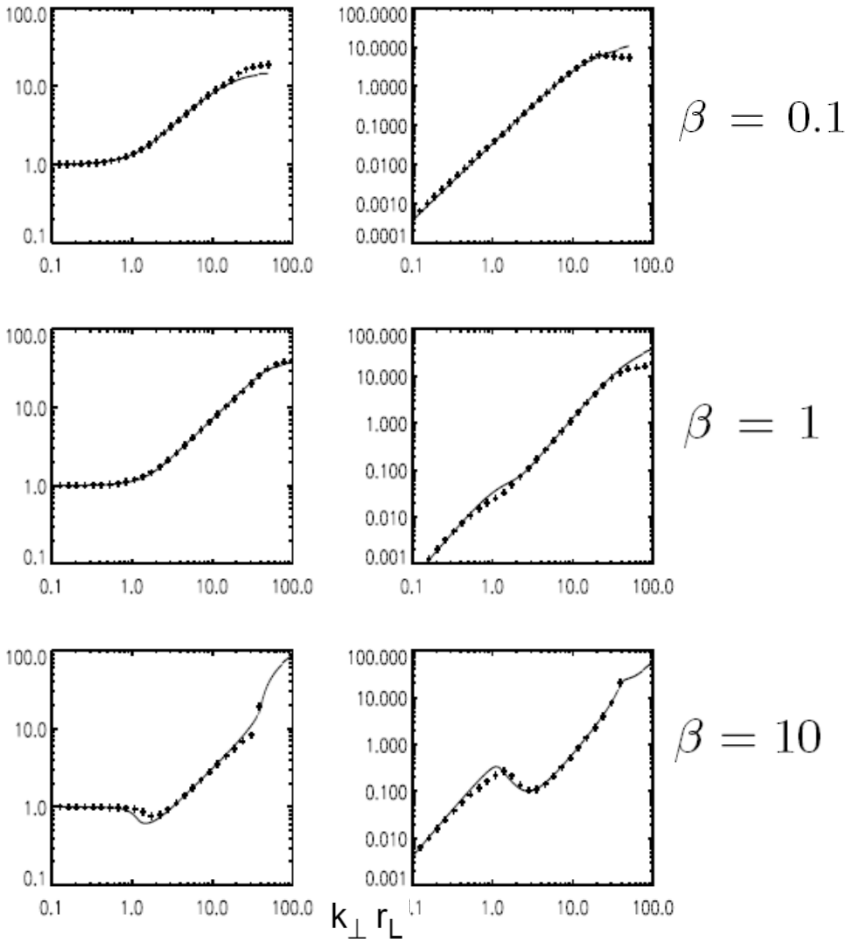

FIG. 2: Normalized frequency $\omega_r/(k_\parallel v_A)$ (left) and damping rate $-\omega_i/(k_\parallel v_A)$ (right) for KAWs with $\theta = \tan^{-1}(1000)$, $\tau = 1$, versus $k_\perp r_L$ for $\beta = 0.1$ (top), $\beta = 1$ (middle), $\beta = 10$ (bottom).

θ=89.9°

Does not capture resonance

oblique propagation

θ≈84° $\theta = \tan^{-1}(10)$

frequency damping rate

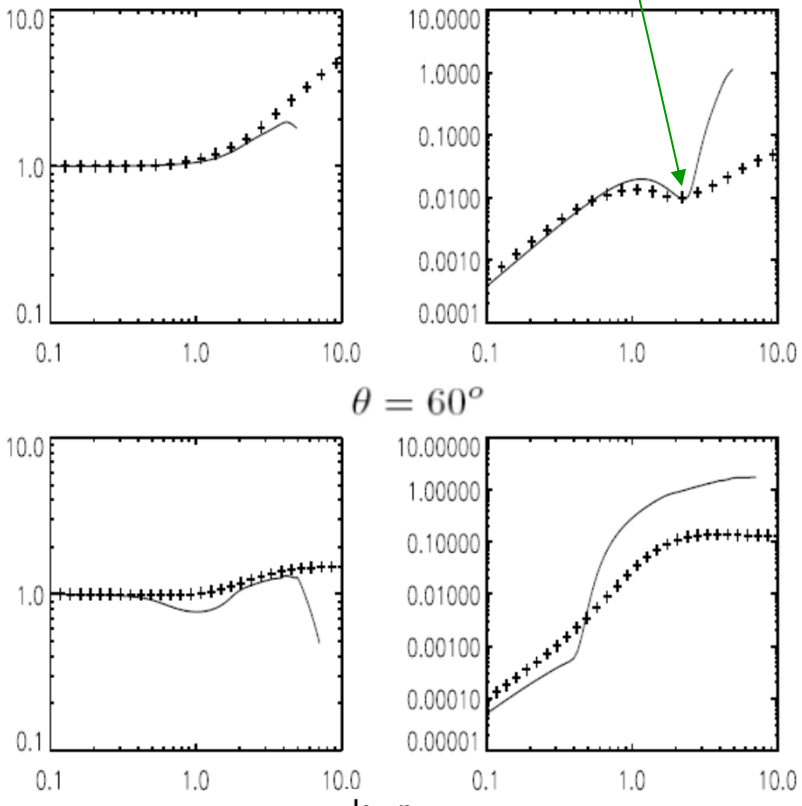

FIG. 3: Normalized frequency $\omega_r/(k_\parallel v_A)$ (left) and damping rate $-\omega_i/(k_\parallel v_A)$ (right) for KAWs with $\tau = 0.01$, $\beta = 1$ versus $k_\perp r_L$ for $\theta = \tan^{-1}(10)$ (top), $\theta = 60^o$ (bottom).

Kinetic Alfvén waves

Meso-Scale Landau fluid

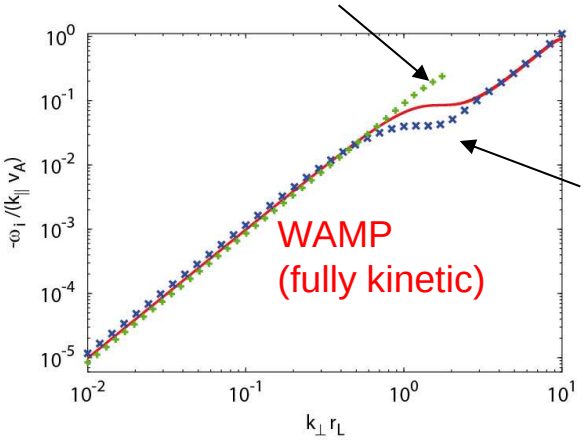

FLR-Landau fluid

KAW, θ=89°

$\beta_{//}=2$
$a_p=a_e=1$
$\tau=1$

Damping rate

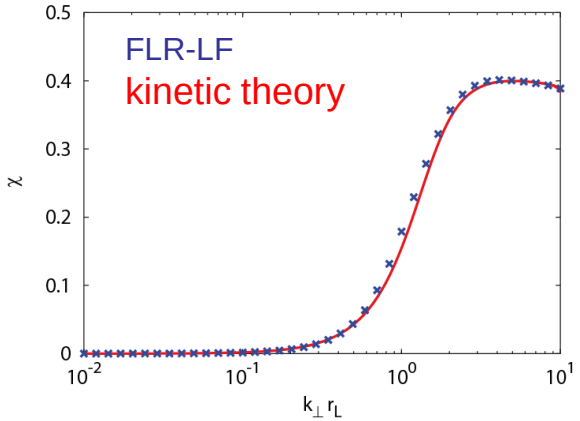

Magnetic compressibility

$$\chi = |b_z|^2/|B|^2$$

electric field

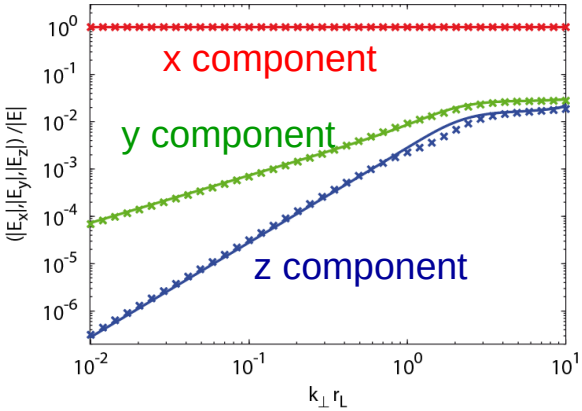

magnetic field

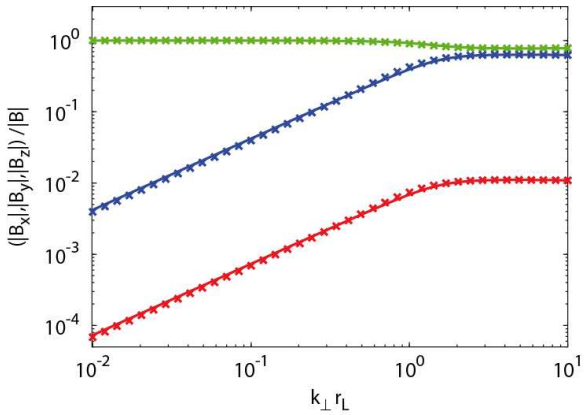

velocity field

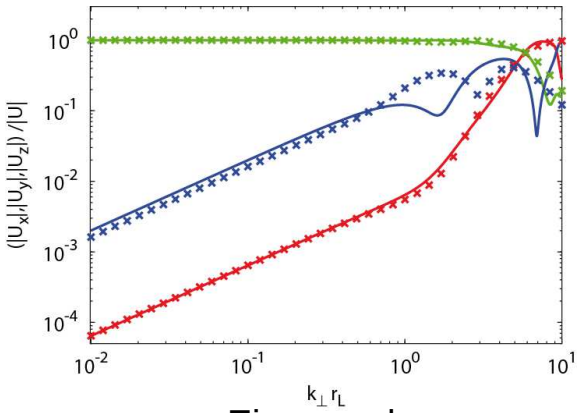

Eigenmode

Meso-Scale Landau fluid is correct up to $k_\perp r_L \approx 1$

Passot et al., PoP 19, 082113, 2012

Comparison FLR-Landau fluid with full kinetics

For large β and angles close to 90°,
the frequency can exceed the ion gyrofrequency without encountering resonance.
In this case, the FLR-Landau fluid remains valid.

real frequency

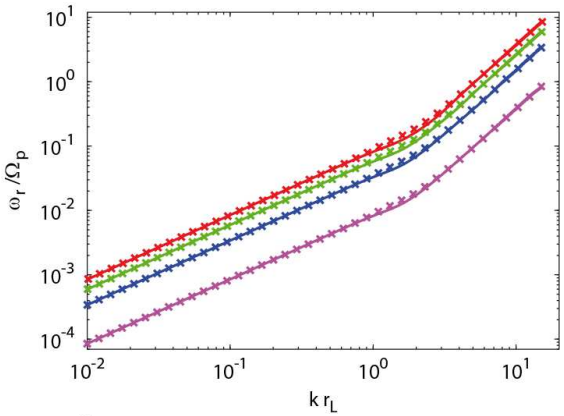

damping rate

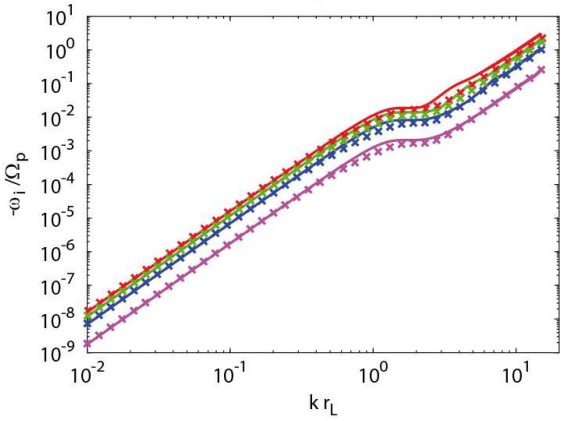

$$\beta = 4.2$$

θ=80° (red), θ=83° (green), θ=86° (blue), θ=89° (magenta)

Comparison FLR-Landau fluid (crosses) with full kinetics (continuous line)

magnetic compressibility: $\chi(k_\perp r_L) = |B_z(k_\perp r_L)|^2/|B(k_\perp r_L)|^2$

electric field polarization: $\mathcal{P} = \mathrm{Arg}(E_y/E_x)/\pi.$ $\begin{cases}\mathcal{P} < 0 & \text{left polarized wave}\\ \mathcal{P} > 0 & \text{right polarized wave}\end{cases}$

propagation angle $\theta = 89.99°$ | $\theta = 60°$

magnetic compressibility | polarization | magnetic compressibility | polarization

polytropic bi-fluid

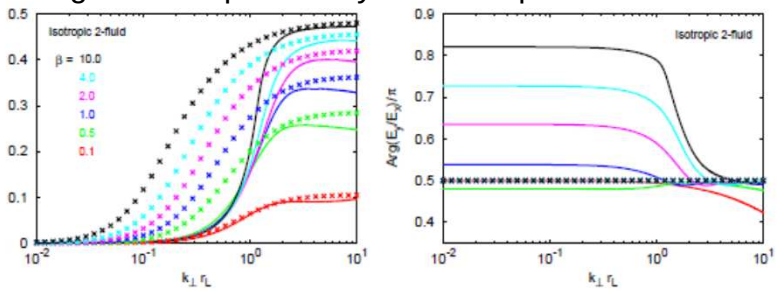

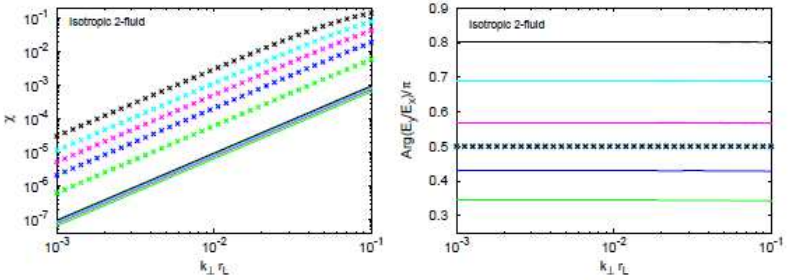

LS-LF

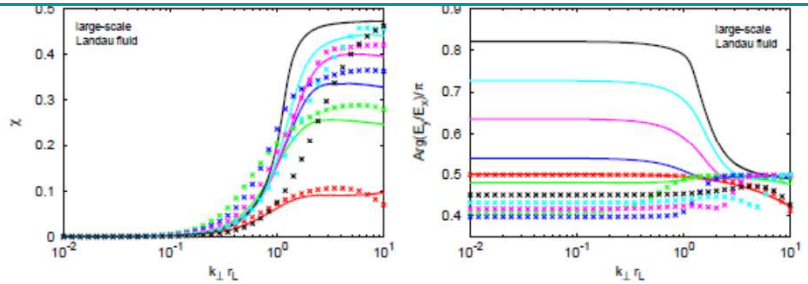

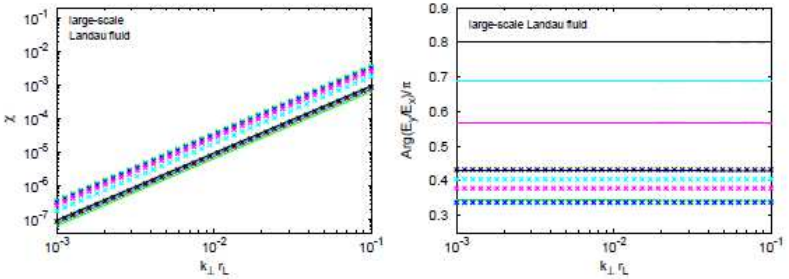

FLR-LF

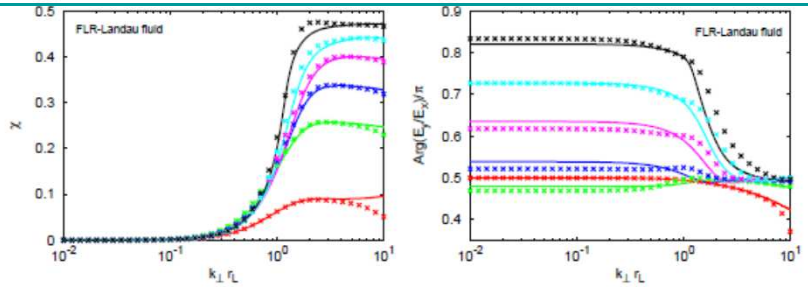

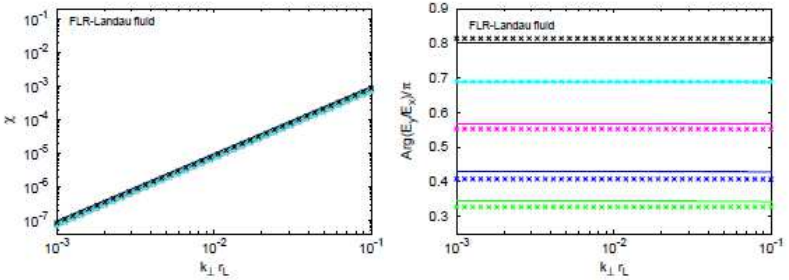

Proton beta is 0.1, 0.5, 1, 2, 4, 10

Polytropic bi-fluid : incorrect even at large scales; Landau damping is not sufficient to reproduce kinetic theory.
FLR-Landau fluid provides an precise agreement with kinetic theory. (*Hunana et al. ApJ, in press).*
Anisotropy of pressure fluctuations alone introduce a major change in wave properties!

The isothermal electron equation of state leads to drastically different results already when $k_\perp \rho \geq 1$

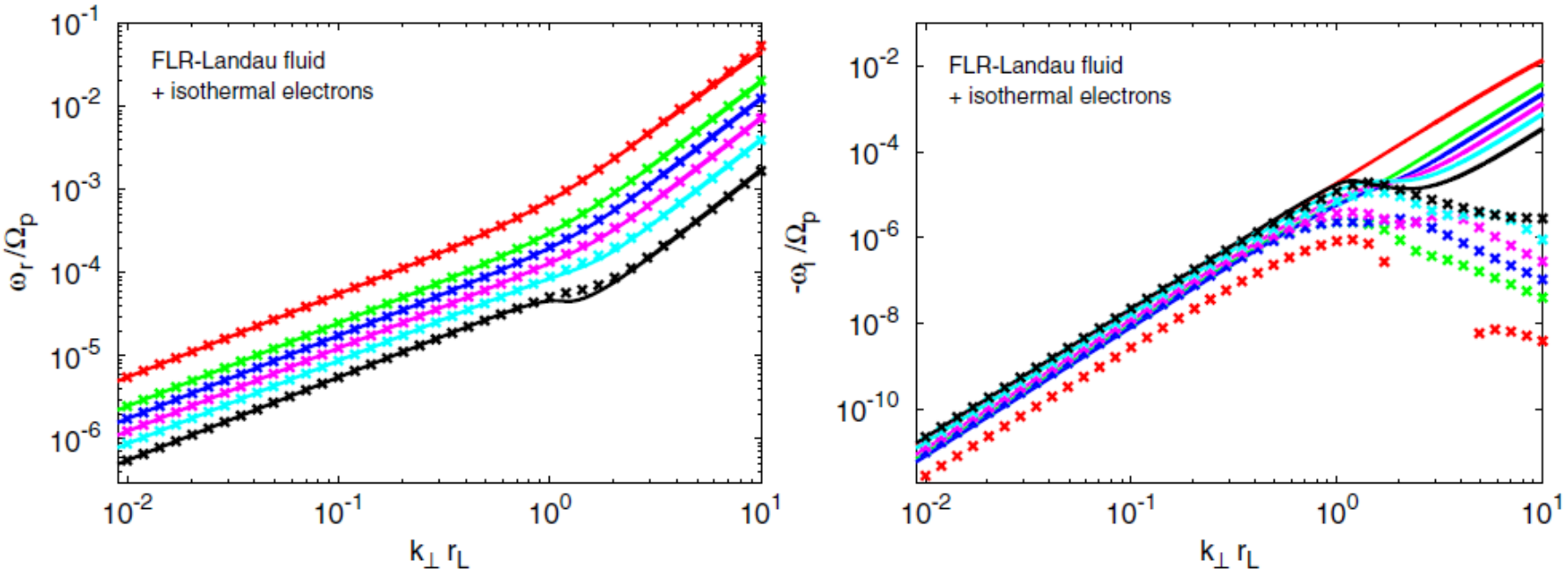

The proton plasma beta is 0.1 (red), 0.5 (green), 1.0 (blue), 2.0 (magenta), 4.0 (cyan), and 10.0 (black).

propagation angle $\theta = 89.99°$

=> caution should be taken with hybrid models

Fast magnetosonic waves

$$\beta = 3,\ \tau = 1,\ a_e = a_p = 1,\ \theta = \pi/2.$$

Ion-cyclotron resonance
is not captured by Landau fluids

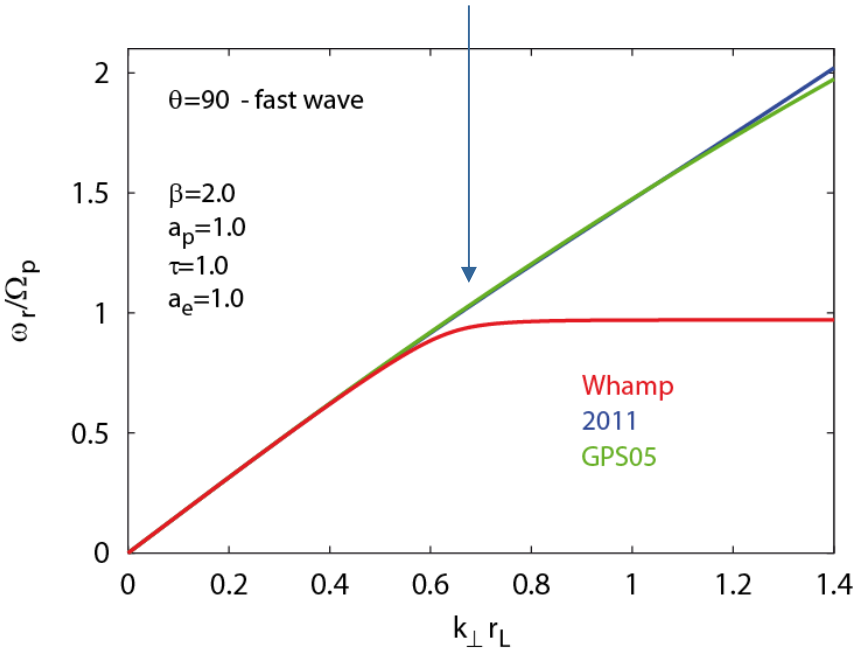

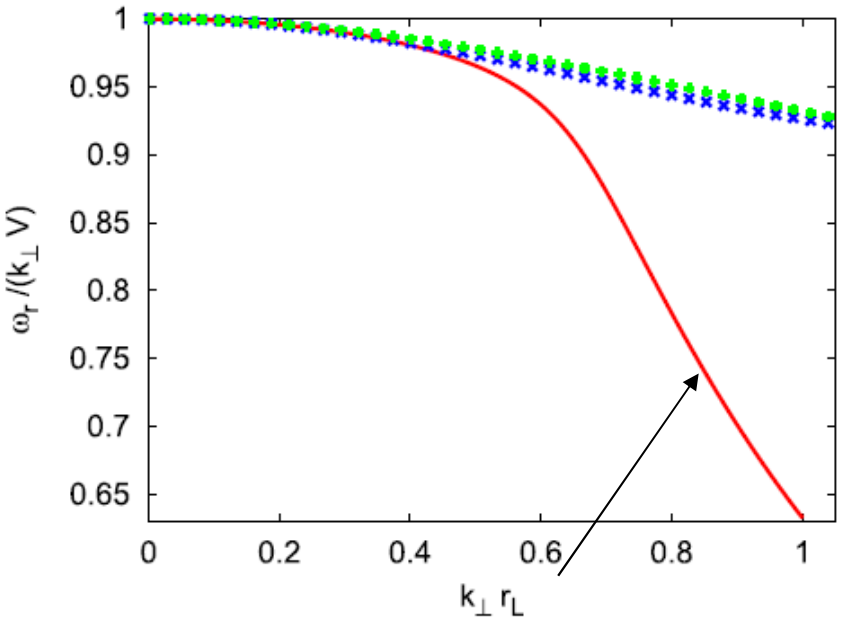

WHAMP

Landau fluids capture fast magnetosonic waves up to the ion cyclotron resonance

Non-modal linear theory:

Transient growth in a homogeneous medium at rest with a uniform magnetic field: it is more accentuated for smaller scales and higher plasma beta.

Camporeale et al. PoP **16**, 030703 (2009) & ApJ **715**:260–270 (2010)

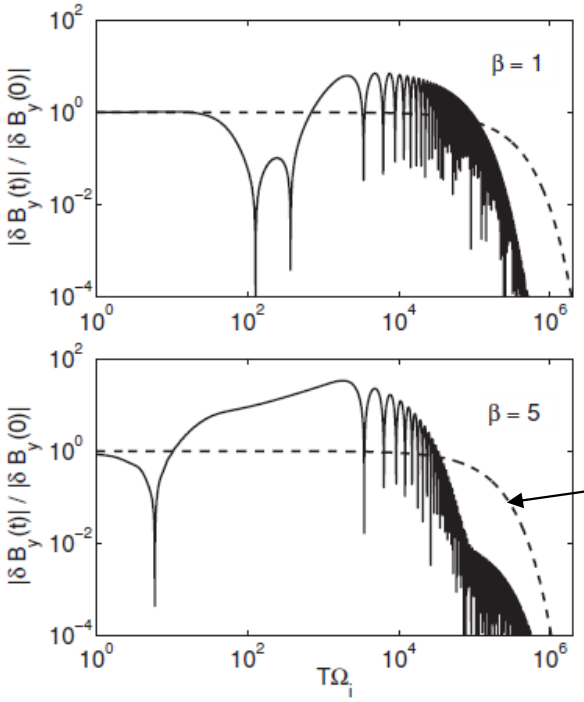

Prediction of modal theory.

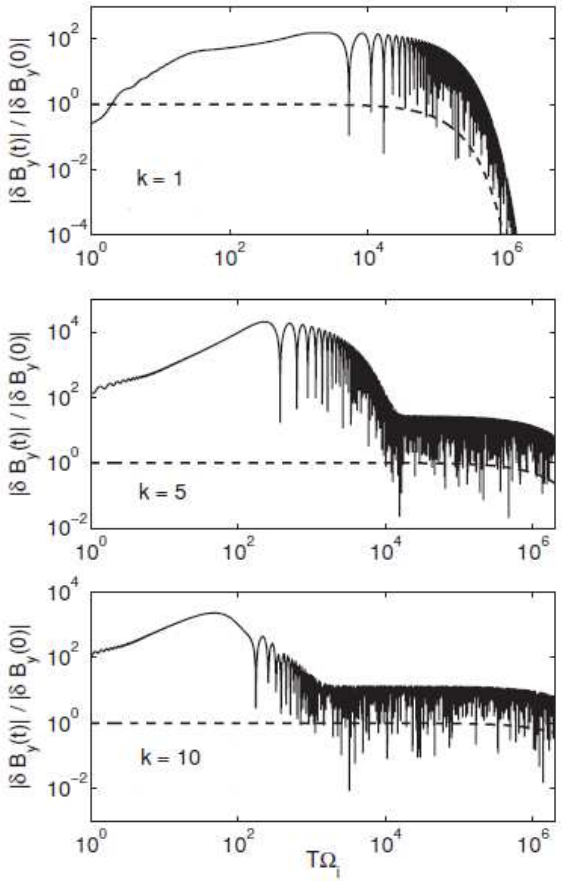

Longer persistence of large perturbations closer to marginal stability (electron oblique firehose, quasi-perpendicular propagation)

$T_\perp / T_\parallel = 0.65, \quad \beta = 5,$

Average for 10 000 random initial perturbations

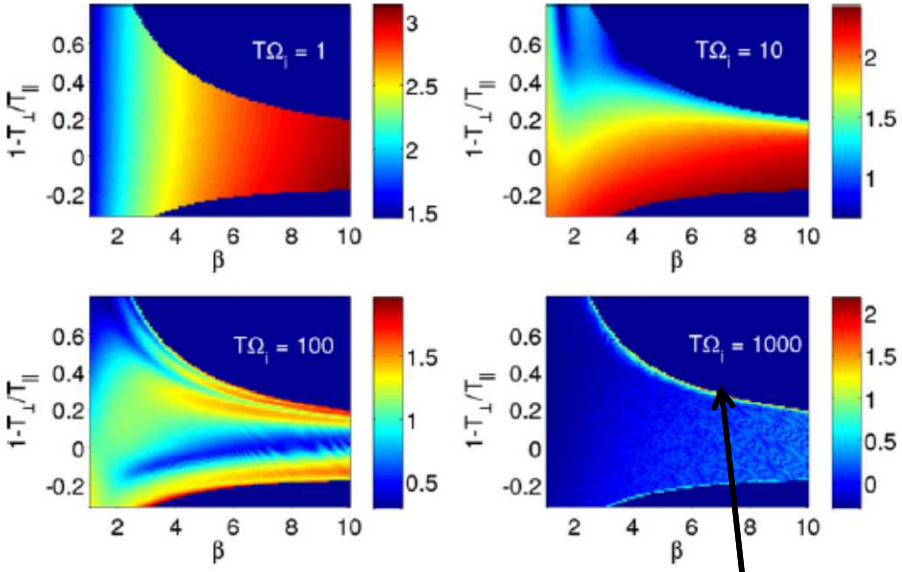

Total norm of state vector

Temperatures refer to electrons

Marginal stability curve

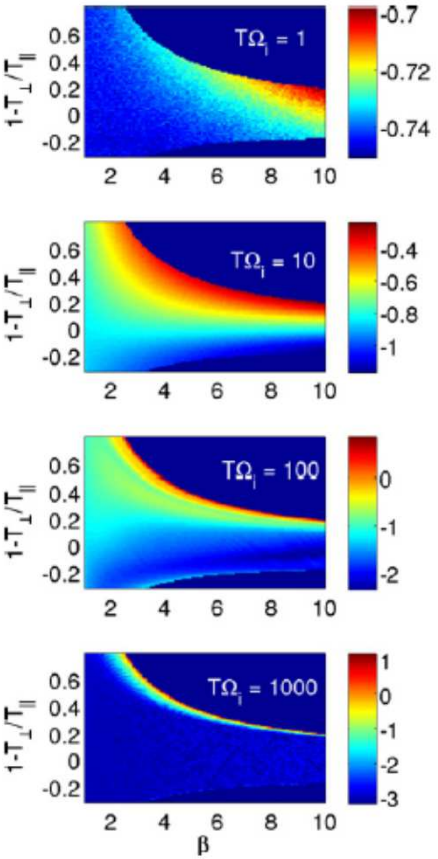

Magnetic fluctuation

Enhanced near stability boundary

In this scenario, a parcel of plasma could experience a “local” marginal stability condition due to a temporary enhanced magnetic fluctuation, and the anisotropy will be reduced in the same way as it is reduced under unstable conditions.

Parallel Alfvén wave dynamics using a simplified Landau-fluid model

Decay instability of parallel Alfvén waves in the long-wavelength limit in 1D

(no dispersion)

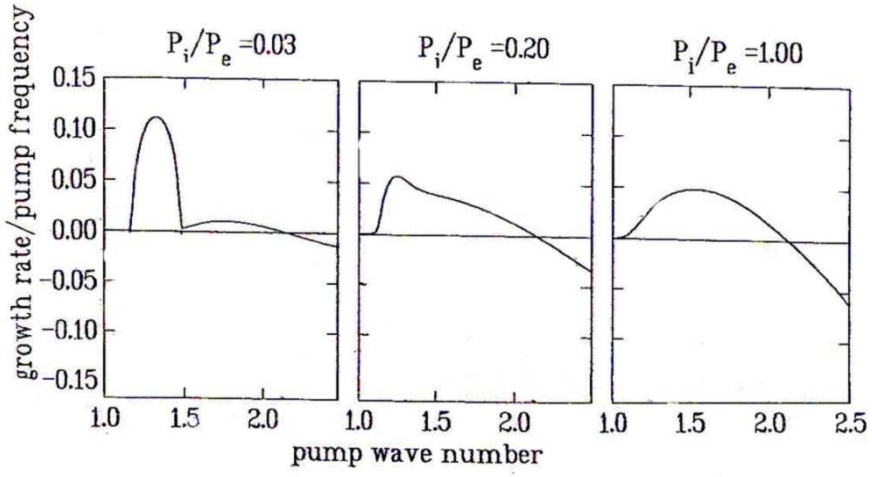

Drift-kinetic analysis (from Inhester 1990)

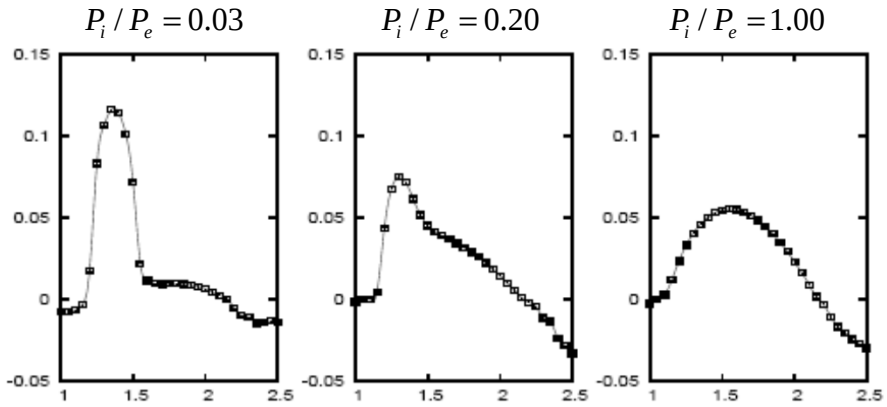

Landau fluid simulation

Maximum growth rates of the density modes versus wavenumber (normalized by the pump wavenumber) resulting from the decay instability of a non dispersive Alfvén wave of amplitude $b_0 = 0.447$ in a plasma with $\beta_{\|p} = 0.3$ and isotropic temperatures such that $T_e^{(0)}/T_p^{(0)} = 33$ (left), $T_e^{(0)}/T_p^{(0)} = 5$ (middle) and $T_e^{(0)}/T_p^{(0)} = 1$ (right).

Reducing electron temperature tends to broaden the spectral range and to reduce the growth rate of the instability.

Decay instability of Alfvén wave produces a forward propagating acoustic wave and a backward Alfvén wave with wavenumber smaller than that of the pump.

In the cas of parametric decay of parallel propagating Alfvén waves
the parallel (perpendicular) temperature is found to increase (decrease).

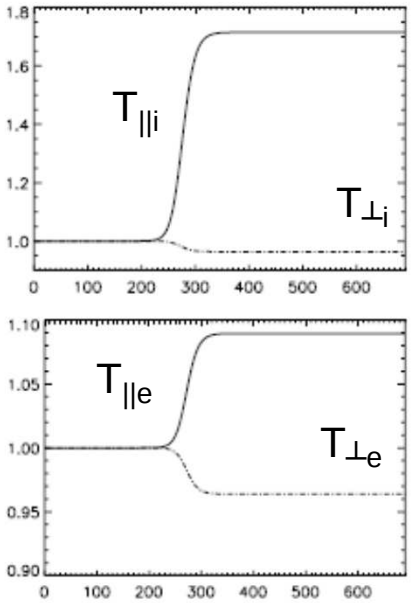

Fig. 3. Time evolution of parallel (solid lines) and transverse (dashed-dotted lines) mean temperatures of the ions (top) and the electrons (bottom) in the run of Fig. 1 (right).

Burgnon et al. **NPG** 11, 609 (2004)

Results consistant with Hybrid PIC simulations of Matteini et al. JGR (2010).

The case of modulational instability is different:

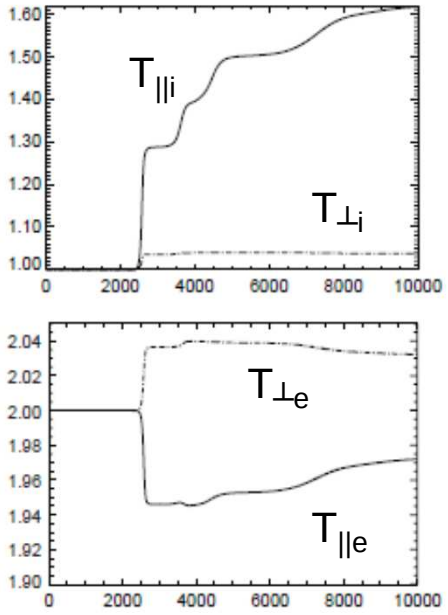

Fig. 10. Time evolution of parallel (solid lines) and transverse (dashed-dotted lines) of the ion (top) and electron (bottom) mean temperatures in the conditions of Fig. 7.

Propagation in a density inhomogeneity in 3D

Electrons are viewed as an (isothermal) fluid with a scalar pressure

- Ion equations *(electron inertia neglected)*

$$\frac{\partial \rho}{\partial t} + \boldsymbol{\nabla} \cdot (\rho \mathbf{u}_p) = 0$$

$$\frac{\partial \mathbf{u}_p}{\partial t} + \mathbf{u}_p \cdot \boldsymbol{\nabla} \mathbf{u}_p + \frac{\beta_p}{2\rho} \boldsymbol{\nabla} \cdot (p_{\perp p} \mathbf{n} + p_{\parallel p} \boldsymbol{\tau} + \boldsymbol{\Pi} + p_e \mathbf{I}) - \frac{1}{\rho} \left[(\mathbf{b} \cdot \boldsymbol{\nabla}) \mathbf{b} - \frac{1}{2} \boldsymbol{\nabla} |\mathbf{b}|^2 \right] = 0$$

$$\frac{\partial \mathbf{b}}{\partial t} = \boldsymbol{\nabla} \times (\mathbf{u}_p \times \mathbf{b}) - \frac{1}{R} \boldsymbol{\nabla} \times \left[\frac{(\boldsymbol{\nabla} \times \mathbf{b}) \times \mathbf{b}}{\rho} \right]$$

$$\frac{\partial p_\perp}{\partial t} + \nabla \cdot (p_\perp \mathbf{u}) + p_\perp \boldsymbol{\nabla} \cdot \mathbf{u} - p_\perp \mathbf{b} \cdot \boldsymbol{\nabla} \mathbf{u} \cdot \mathbf{b} + \boldsymbol{\nabla} \cdot (q_\perp \mathbf{b}) + q_\perp \boldsymbol{\nabla} \cdot \mathbf{b} = 0$$

$$\frac{\partial p_\parallel}{\partial t} + \nabla \cdot (\mathbf{u} p_\parallel) + 2 p_\parallel \mathbf{b} \cdot \boldsymbol{\nabla} \mathbf{u} \cdot \mathbf{b} + \boldsymbol{\nabla} \cdot (q_\parallel \mathbf{b}) - 2 q_\perp \boldsymbol{\nabla} \cdot \mathbf{b} = 0$$

(non gyrotropic heat flux contributions neglected)

where $\mathbf{n} = \mathbf{I} - \widehat{\mathbf{b}} \otimes \widehat{\mathbf{b}}$, $\boldsymbol{\tau} = \widehat{\mathbf{b}} \otimes \widehat{\mathbf{b}}$, $\widehat{\mathbf{b}} = \mathbf{B}/B$, $R = L/l_i$, $\beta = 8\pi p^{(0)}_{\parallel p}/B_0^2$

- Third order momentum closure

Hilbert transform (signature of Landau damping)

$$\left(\frac{d}{dt}+\frac{\sqrt{\pi\beta_p}}{4(1-\frac{3\pi}{8})}\mathcal{H}\partial_z\right)q_{\parallel}=\frac{1}{1-\frac{3\pi}{8}}\frac{\beta_p}{2}\partial_z(p_{\parallel}-\rho)$$

$$\mathcal{H}f(z)=\frac{1}{\pi}VP\int_{-\infty}^{+\infty}\frac{f(z')}{z-z'}dz'$$

$$\left(\frac{d}{dt}-\frac{\sqrt{\pi\beta_p}}{2}\mathcal{H}\partial_z\right)q_{\perp}=\frac{\beta_p}{2}\frac{T^{(0)}_{\perp p}}{T^{(0)}_{\parallel p}}\partial_z\left[\left(1-\frac{T^{(0)}_{\perp p}}{T^{(0)}_{\parallel p}}\right)|b|-\left(\frac{T^{(0)}_{\parallel p}}{T^{(0)}_{\perp p}}p_{\perp}-\rho\right)\right]$$

- Ion gyroviscous tensor

$$\Pi_{xx}=-\Pi_{yy}=-\frac{p_{\perp}}{2R}(\partial_y u_x+\partial_x u_y)\,,\qquad \Pi_{xy}=\Pi_{yx}=-\frac{p_{\perp}}{2R}(\partial_y u_y-\partial_x u_x)$$

$$\Pi_{yz}=\Pi_{zy}=\frac{1}{R}[2p_{\parallel}\partial_z u_x+p_{\perp}(\partial_x u_z-\partial_z u_x)]$$

$$\Pi_{xz}=\Pi_{zx}=-\frac{1}{R}[2p_{\parallel}\partial_z u_y+p_{\perp}(\partial_y u_z-\partial_z u_y)]\,,\qquad \Pi_{zz}=0$$

Comparison between Landau fluid and hybrid PIC simulations

Landau fluid PIC

Propagation of an Alfvén wave in a density inhomogeneity (parallel high density channel of small amplitude)

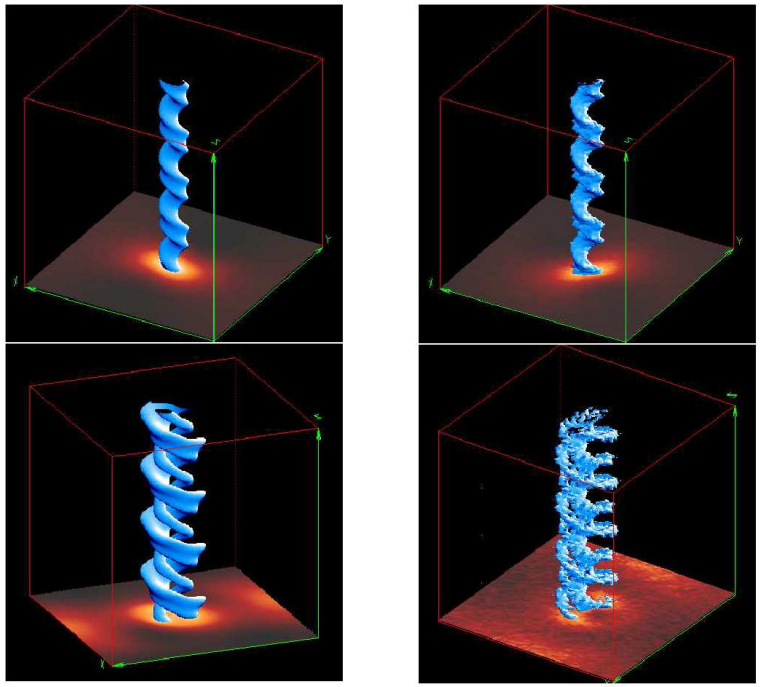

At larger amplitude

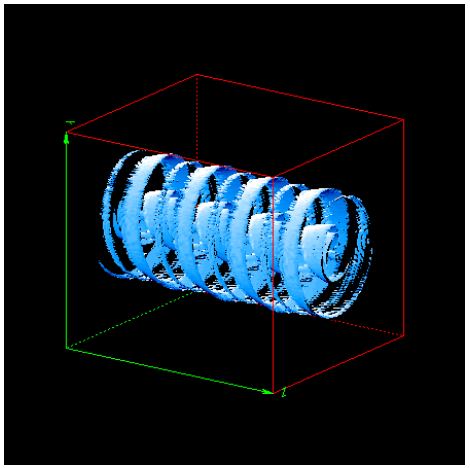

Borgogno et al. NPG 16, 275 (2009)

$$T_e / T_p = 1/30$$

$$\beta_p = 0.3 \quad \beta_e = 0.01$$

Decay simulations in 3D: Reduction of compressibility and parallel transfer by Landau damping

P. Hunana, D. Laveder, T. Passot, P.L. Sulem, D. Borgogno, ApJ **743**:128 (2011)

3D MS-Landau fluid simulations in a turbulent regime

(simplified model) (*Hunana, Laveder, Passot, Sulem & Borgogno, ApJ* ***743,*** *128, 2011).*

Freely decaying turbulence (temperatures remain close to their initial values)

- Isothermal electrons
- Initially:
  - no temperature anisotropy;
  - equal ion and electron temperatures
  - incompressible velocity.

Pseudo-spectral code
Resolution: 128^3 (with small scale filtering)

Size of the computational domain: 32 π inertial lengths in each direction
Initially, energy on the first 4 velocity and magnetic Fourier modes $kd_i = m/16$ (m=1,…,4)
with flat spectra and random phase.

Comparison of MS-Landau fluids and Hall-MHD simulations

Compressibility reduction by Landau damping

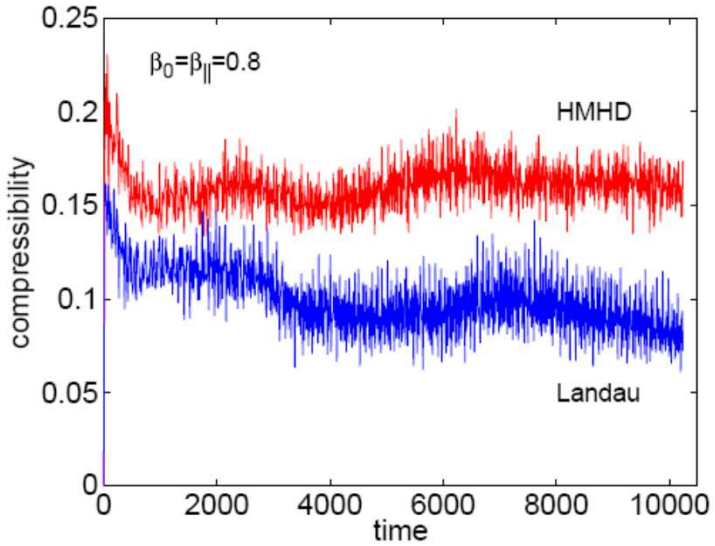

FIG. 6: Compressibility for Hall-MHD (red line) and FLR-Landau fluid (blue line) evaluated as $(\sum_k |\boldsymbol{k}\cdot\boldsymbol{u}_k|^2/|\boldsymbol{k}|^2)/\sum_k |\boldsymbol{u}_k|^2$ for $\beta_0 = \beta_{||} = 0.8$. Both regimes start with the identical initial condition where the velocity field is divergence free. The figure shows that the compressibility is clearly inhibited in the Landau fluid simulation.

Important in solar wind context: Although solar wind is a fully compressible medium, the turbulent fluctuations behave as is there were weakly compressible.

Spectral anisotropy

Hall-MHD

FLR-Landau fluid

Transverse directions

Parallel direction

Kinetic energy

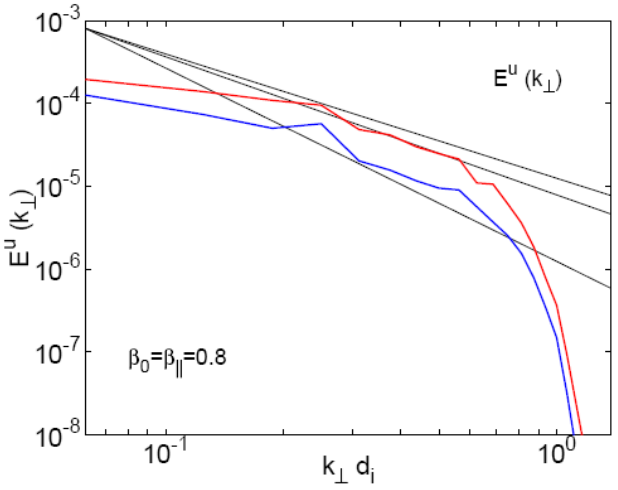

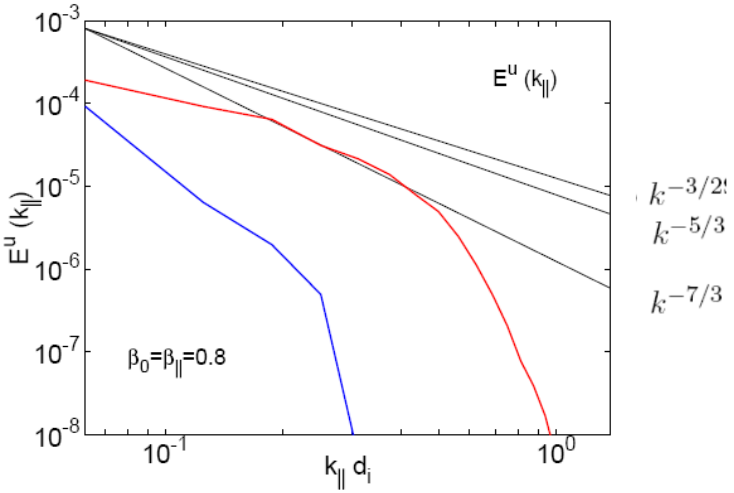

Magnetic energy

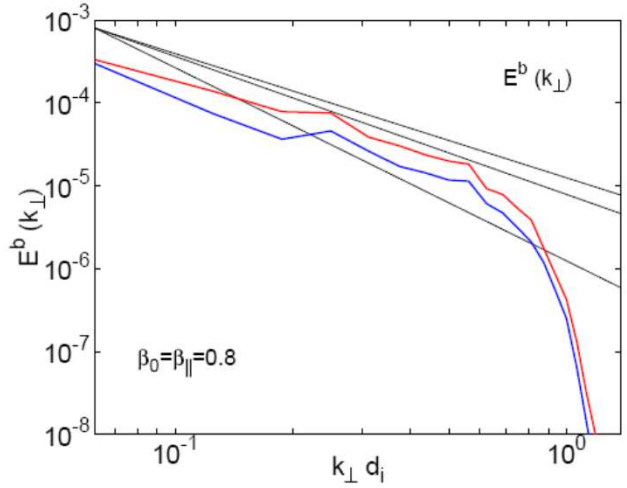

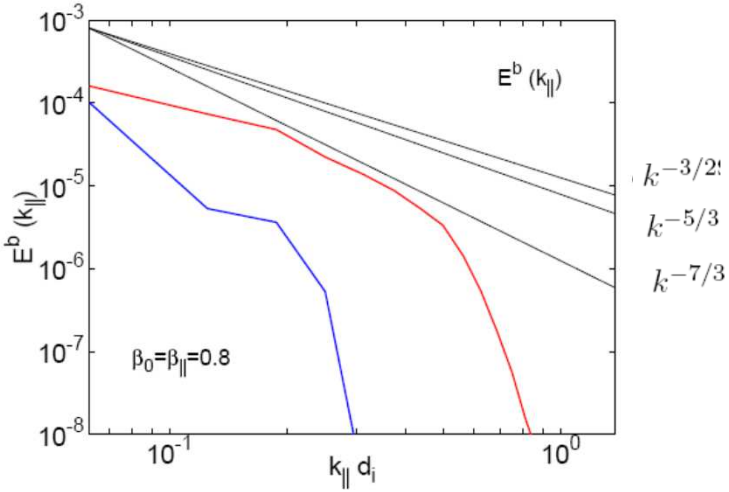

Strong reduction of the parallel transfer

Damping of slow modes

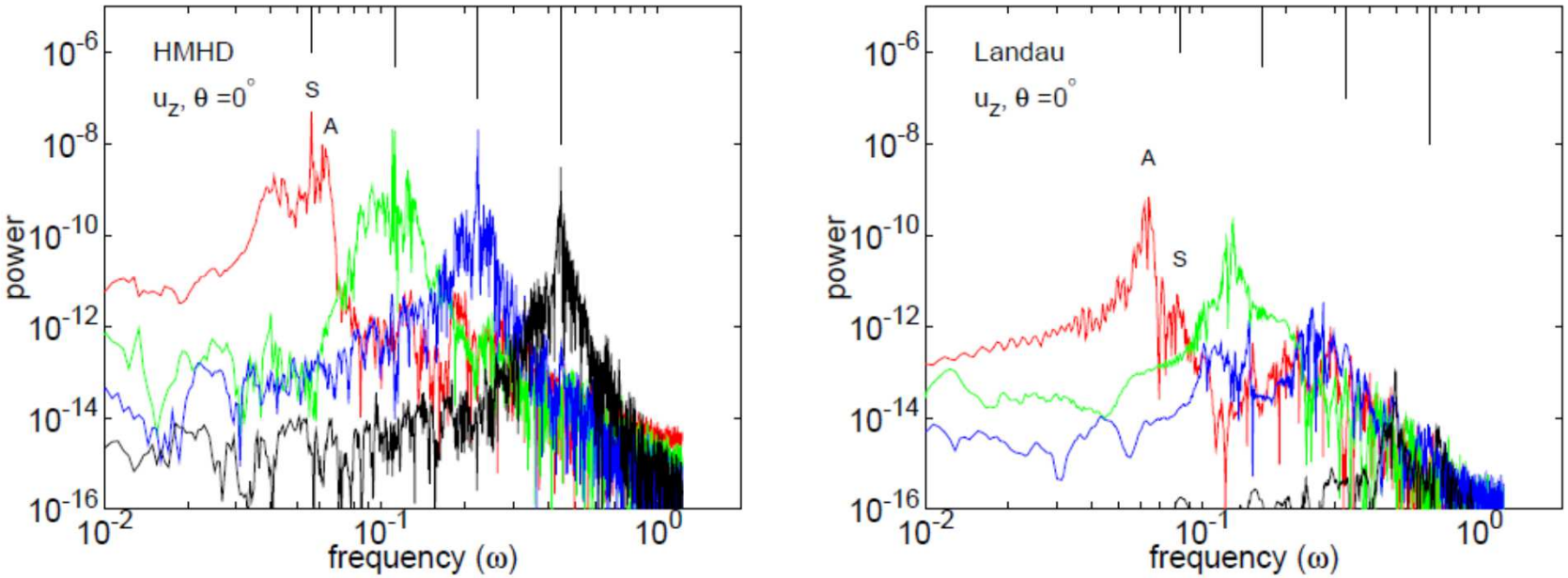

Strong damping of sound waves in oblique directions as well, but not in the perpendicular one.

Simulations of the development of temperature anisotropy and its limitation by micro-instabilities

D. Laveder, L. Marradi, T. Passot, and P. L. Sulem, GRL **38**, L17108 (2011).

"In a number of systems such as the solar corona and the solar wind, ions are observed to undergo perpendicular heating, despite the fact that most of the fluctuation energy is believed to be in the form of low-frequency kinetic Alfvén wave fluctuations. Determining the cause of such perpendicular heating is one of the critical unsolved problem in the study of space and astrophysical turbulence".

(Report of the Workshop on Research Opportunity in Plasma Astrophysics, Princeton, January 2010)

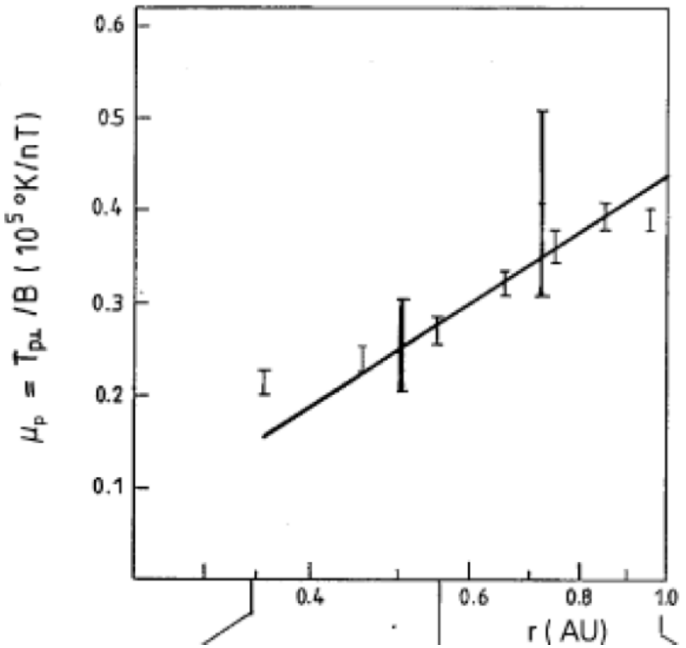

Proton magnetic moment versus the heliocentric distance *(Marsch, Living Review Solar Phys., 2006)*

Non-resonant heating:

Simulation of perpendicular ion heating under the action of given randomly phased KAW with wavelength comparable to the ion Larmor radius on particles for $\beta \lesssim 1$

*(Chandran et al. ApJ **720**, 503, 201 see also Bourouaine, 2008)*

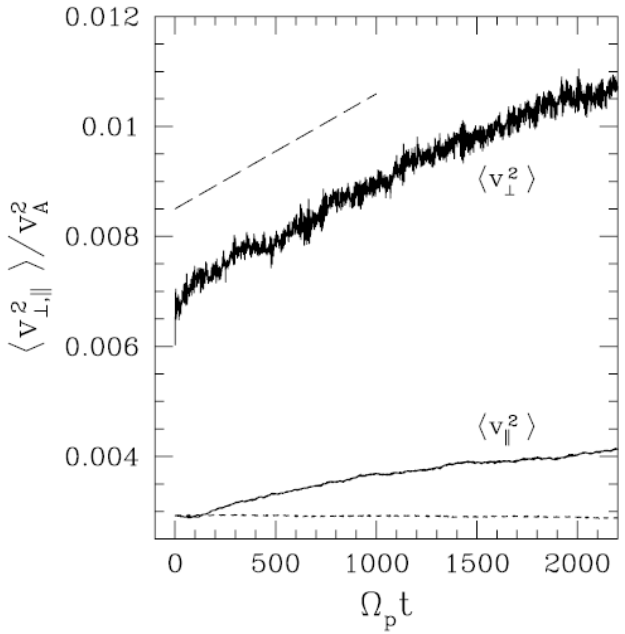

Need for a fully nonlinear approach.

Parameters of the 1D FLR-Landau fluid simulations:

- Angle of propagation: 80^o with respect to the ambient magnetic field

- White noise in time random driving around k_{inj}, applied on the perpendicular velocity component (u_y) each time the sum of kinetic and magnetic energy falls below a given threshold: it is intended to simulate the injection of energy from the end of the solar wind Alfvén wave cascade.

  Resulting root mean square of the transverse magnetic field fluctuations is of the order of 0.12 times the magnitude of the ambient field (realistic for the solar wind)

- Isotropic initial temperatures; various parallel proton β.

- Size of the domain L measured in units of ion inertial length

- Number of grid points: typically N=256 (after partial desaliazing).

- No artificial dissipation is added.

Fixing k_{inj}/k_p=0.087 (relatively small scale) and varying β (thus changing the domain size)

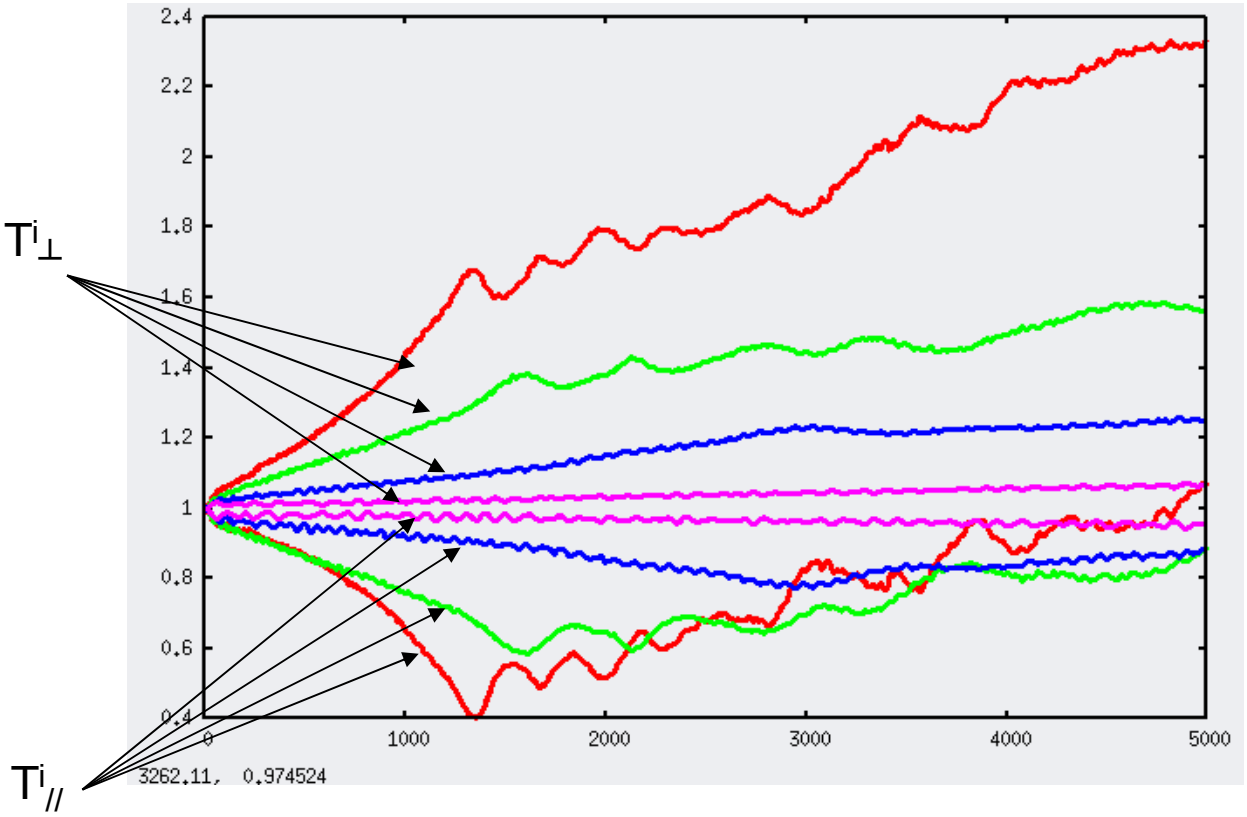

β=0.6

β=1.2

β=2.4

β=9.6

Red: β=0.6, L=12 π
Green: β =1.2, L=16 π
Blue: β =2.4, L=22 π
Pink: β =9.6, L=144 π

Time variation of the (space averaged) ion temperatures

Perpendicular heating and (early time) parallel cooling of ions, with a larger efficiency as β is reduced

(in agreement with simulations of the action of prescribed KAW, *Chandran et al. ApJ 2010)*

With injection at larger scales, there is a critical value of β, below which parallel ion heating and above which perpendicular heating dominates.

Efficient parallel electron heating at small β

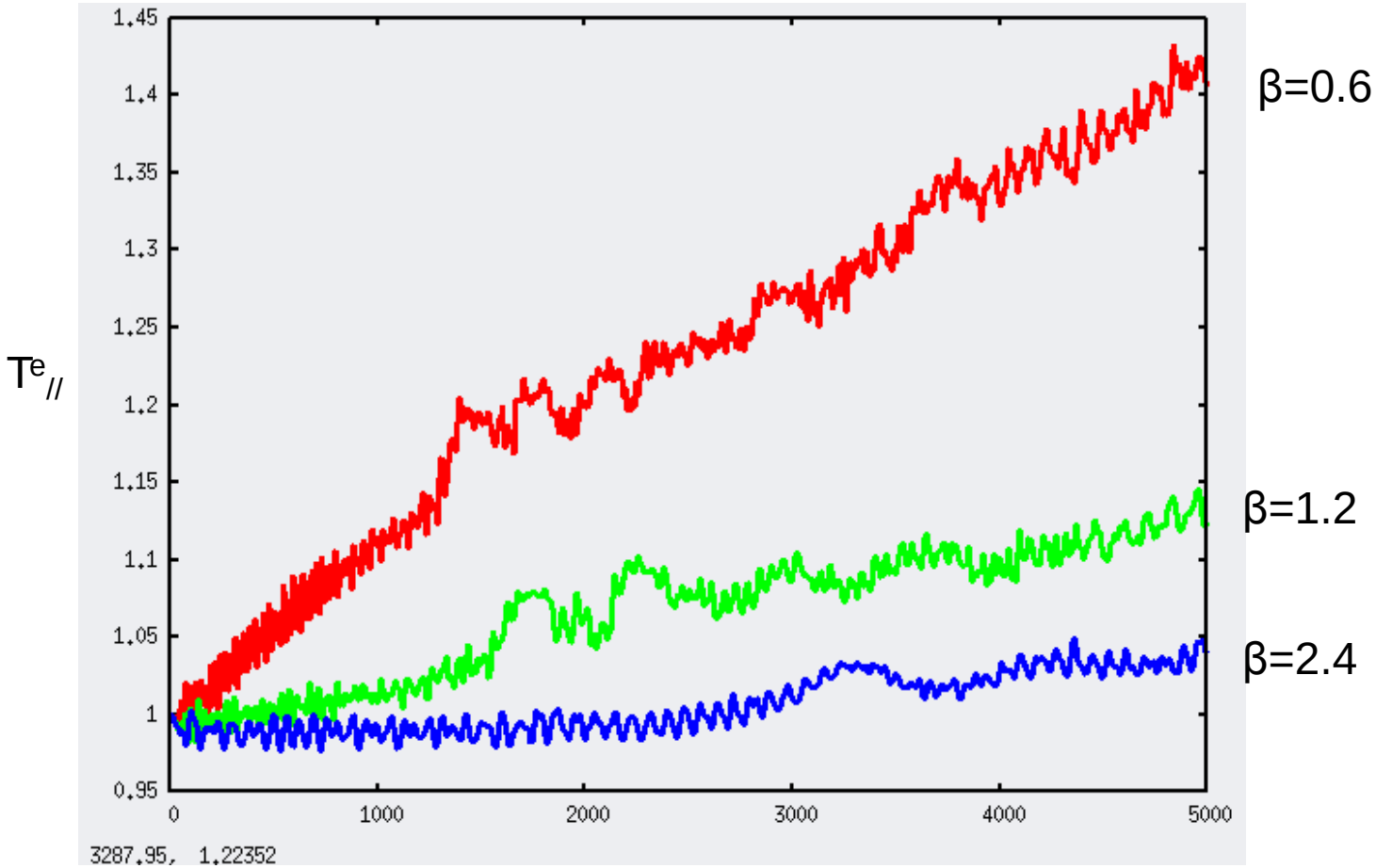

Parallel electron temperature (same conditions)

Parallel cooling β=0.6

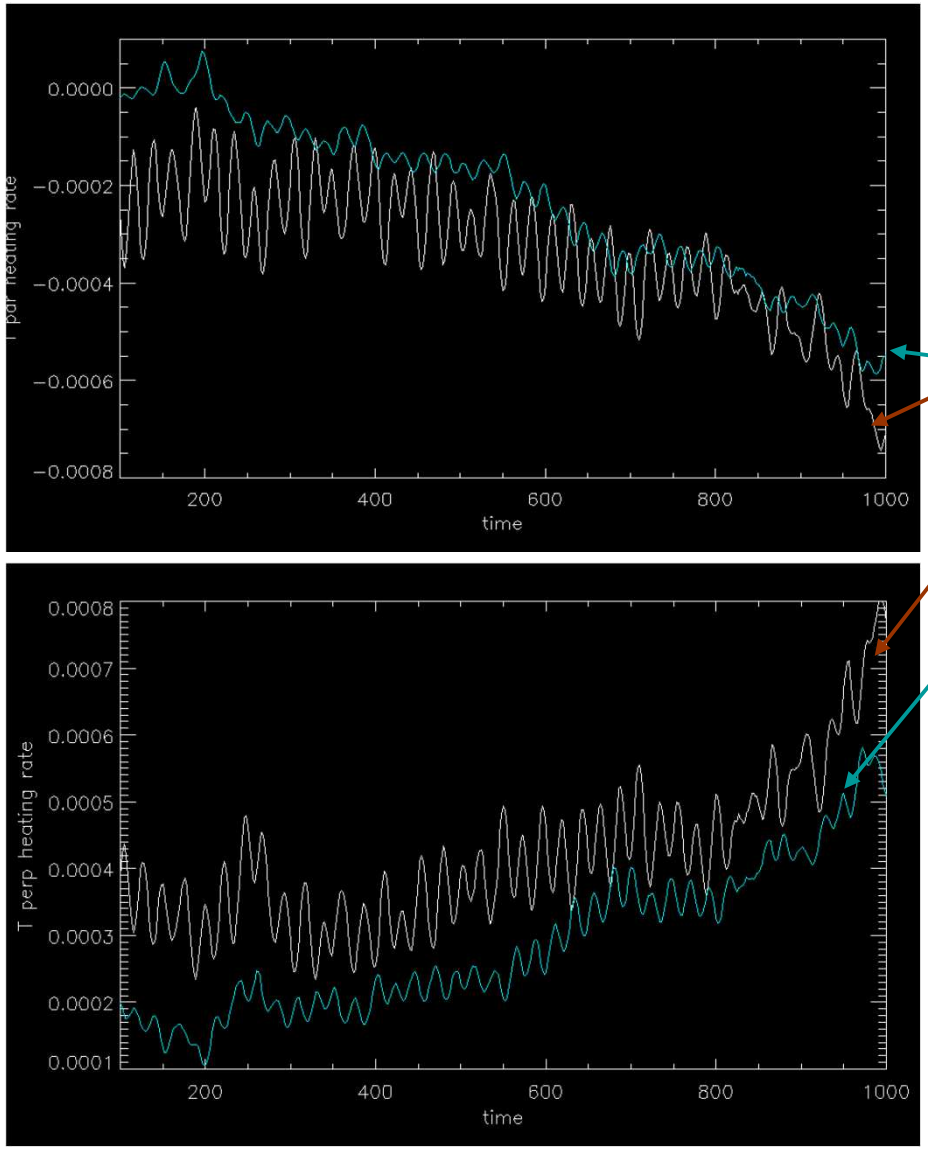

Perpendicular heating

Origin of heating/cooling:

Dominant FLR contributions:
more important close to mirror threshold

total temperature variation

FLR contributions

Space-averaged magnetic moment per unit mass

Hall term

nongyrotropic pressure

$$\partial_t\left(\frac{p_\perp}{|b|}\right)+\nabla\cdot\left(\frac{p_\perp\vec{u}}{|b|}+\frac{q_\perp\widehat{b}}{2|b|}\right)=$$

$$\frac{p_\perp}{|b|^2}\widehat{b}\cdot\left[\nabla\times\left(\frac{m_pc}{\rho e}\left(\frac{\vec{j}\times\vec{b}}{c}-\nabla\cdot\mathbf{p}_e\right)\right)\right]$$

$$-\frac{1}{2|b|}(\nabla_\perp\cdot\vec{S}_\perp^{\perp})-\frac{1}{2|b|}\left(tr(\mathbf{\Pi}\cdot\nabla\vec{u})^s-(\mathbf{\Pi}\cdot\nabla\vec{u})^s:\boldsymbol{\tau}+\mathbf{\Pi}:\frac{d\boldsymbol{\tau}}{dt}\right)$$

nongyrotropic heat flux

dominant contribution

Both parallel and perpendicular heat fluxes contribute to the variation of $\frac{|b|^2p_\parallel}{\rho^2}$

Evolution of the mean temperatures

Eartly time:
heating of perpendicular proton temperature and cooling of parallel proton temperature associated with low frequency modes.

Growth of ion temperatures: $T^i_\perp > T^i_{//}$
More moderate growth of electron temperatures: $T^e_\perp < T^e_{//}$

When mirror modes are linearly damped, $\gamma_k < 0$ dynamics is governed by quasi-linear theory (*Shapiro and Shevchenko* [1964])
(when prescribing a bi-Maxwellian ion distribution function)

Leads to :
- growth of perpendicular ion temperature
- decrease of parallel ion temperature

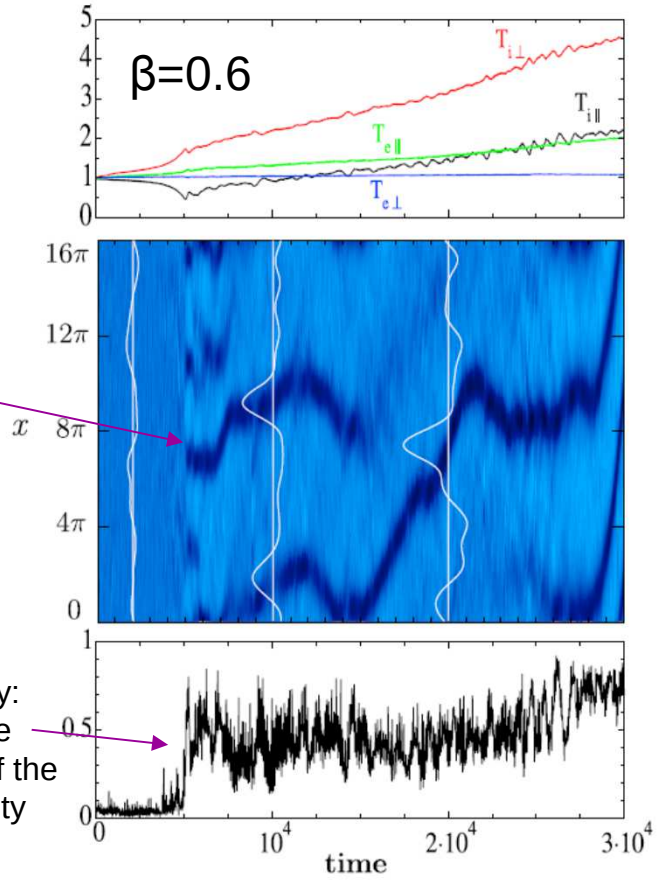

Development of the mirror instability

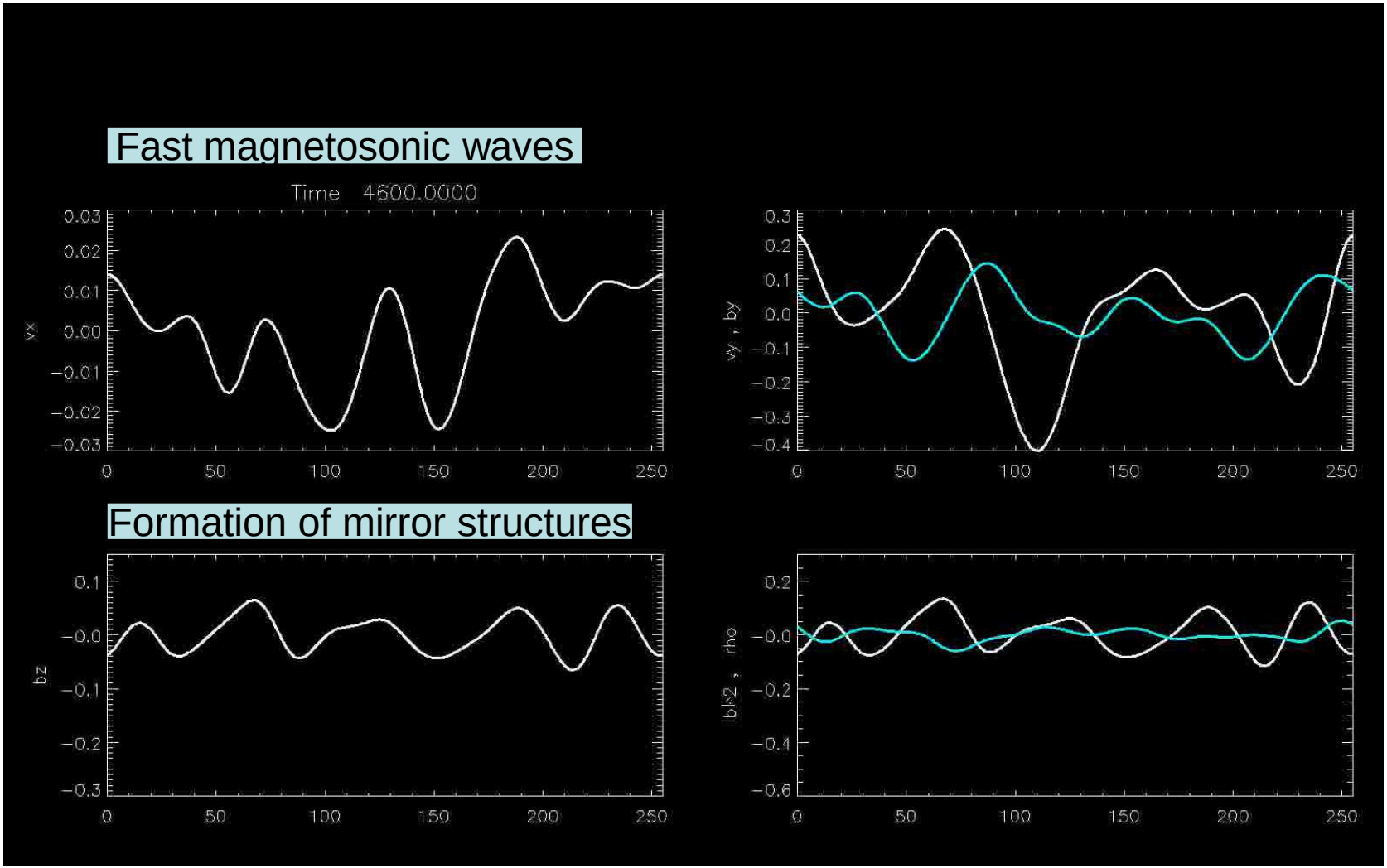

Mirror structures from initial random noise

Using the full model in 1D

$$T_{//e}/T_{//p} = 0.05, \quad T_{\perp e}/T_{//e} = 1, \quad \cos\theta = 0.2$$

$$t = 2000\Omega_p^{-1}$$

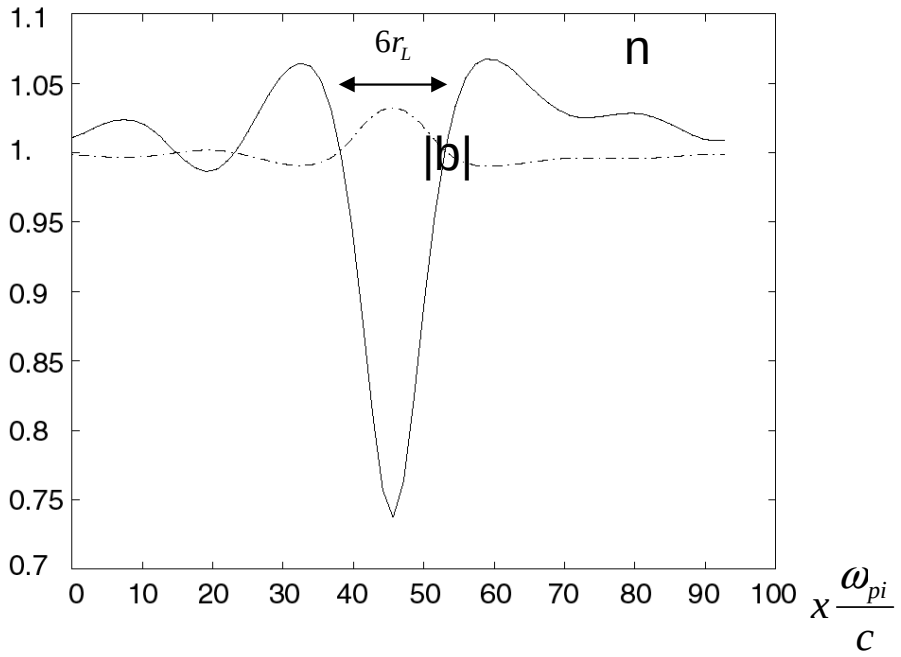

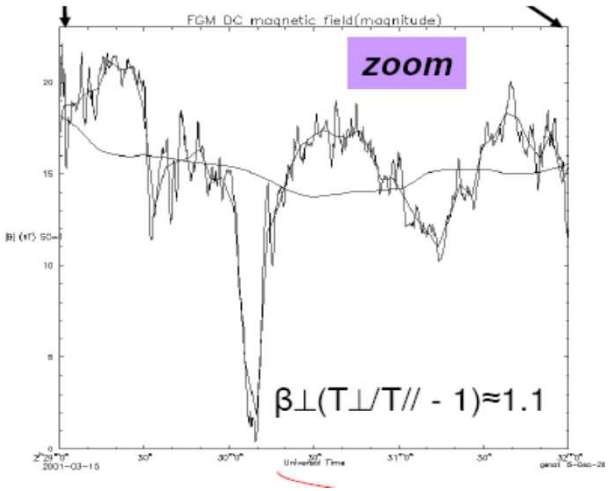

Cluster observations
(Génot et al.)

Formation of static magnetic holes

$$\beta_{//p} = 5, \quad T_{\perp p}/T_{//p} = 1.5$$

The temperature anisotropy is constrained by the mirror instability

Distance to mirror threshold:

Pantellini & Schwartz, JGR **100**, 3539 (1995); Pokhotelov et al. JGR **105**, 2393 (2000), Hellinger PoP 14, 082105 (2007); Kuznetsov, Passot & Sulem, PoP Letter (2012)

$$\Gamma = \beta_{i\perp}\left(\frac{T_{i\perp}}{T_{i\parallel}} - 1\right) + \beta_{e\perp}\left(\frac{T_{e\perp}}{T_{e\parallel}} - 1\right) - 1 - \frac{\left(\frac{T_{i\perp}}{T_{i\parallel}} - \frac{T_{e\perp}}{T_{e\parallel}}\right)^2}{2\left(\frac{1}{\beta_{i\parallel}} + \frac{1}{\beta_{e\parallel}}\right)}$$

The same amount of exchanged thermal and non thermal energy leads to lower temperature change at larger β.

Also more magnetosonic waves at small β, leading to a greater distance to threshold and more oscillations.

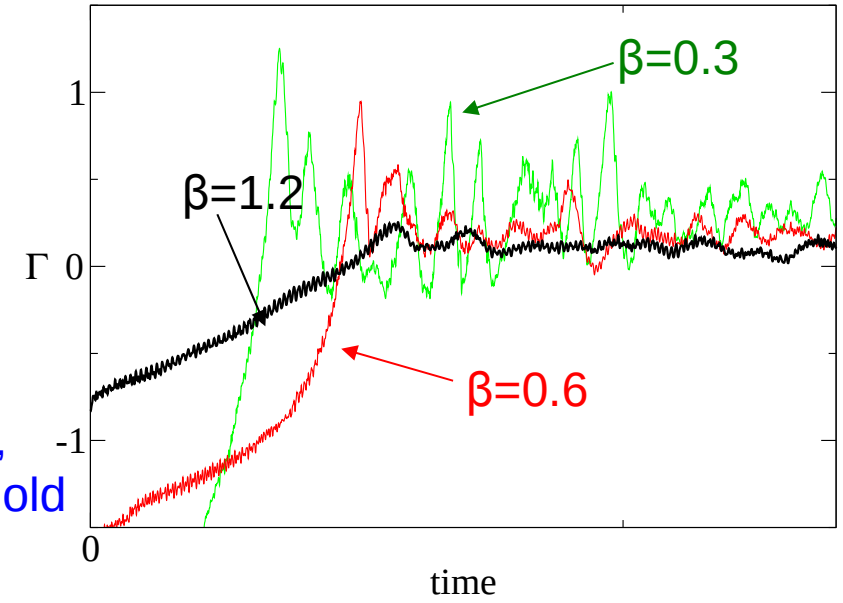

Influence of β, keeping constant $k_{inj}\,\rho_L$

Comparison with solar wind data

A large majority of the observational measurements in the case of a predominant ion perpendicular heating are limited from above by the curve

$$T_{\perp i}/T_{\parallel i} - 1 - a/(\beta_{\parallel i} - \beta_0)^b = 0$$

$$a = 0.77,\ b = 0.76 \text{ and } \beta_0 = -0.016$$

that fits the contour associated with the growth rate $\gamma = 10^{-3}\Omega_i$ of the mirror instability in linear kinetic computations assuming bi-Maxwellian ions and isothermal electrons.

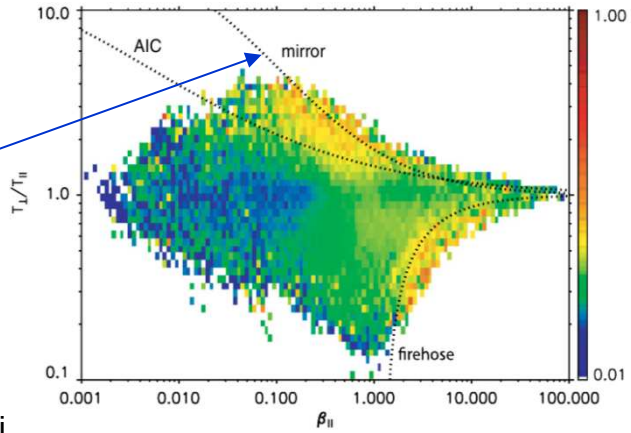

Solar wind data

*Bale et al. PRL **103**, 21101 (2009)*

FLR-Landau fluid simulations:

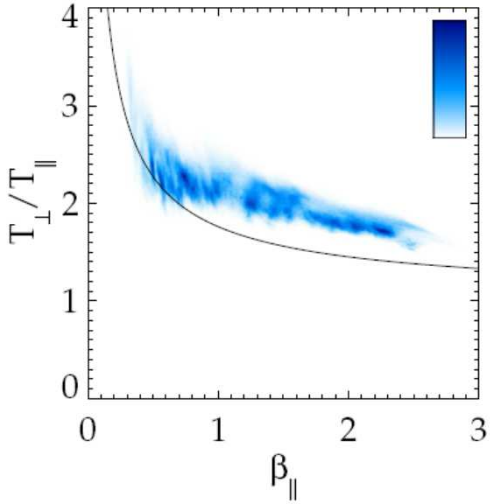

Points: local values of (β// , $T_\perp / T_{//}$) in the simulation at β=0.6

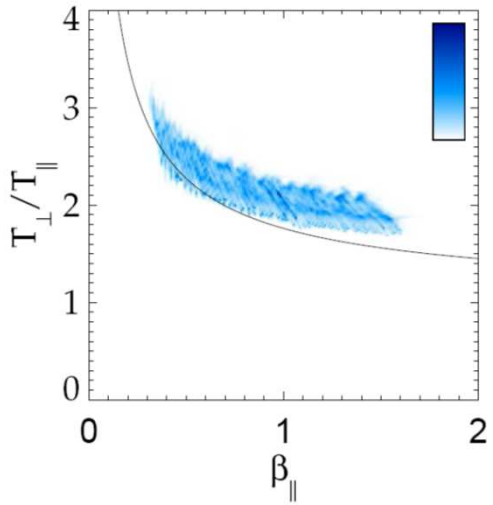

Same, when the energy threshold is divided by a factor 16

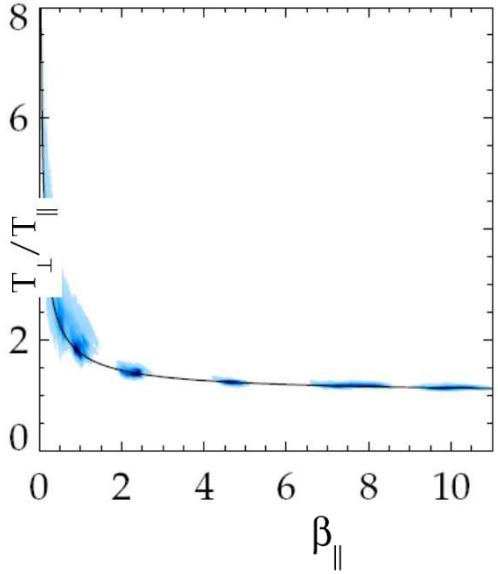

Collecting points from several runs starting at various values of β: the plasma does not enter the unstable range.

Influence of weak collisions

BGK collision operator is included in the Vlasov equation, leading to linear and nonlinear additional contributions in the moment equations (see Green, PoF 1973)

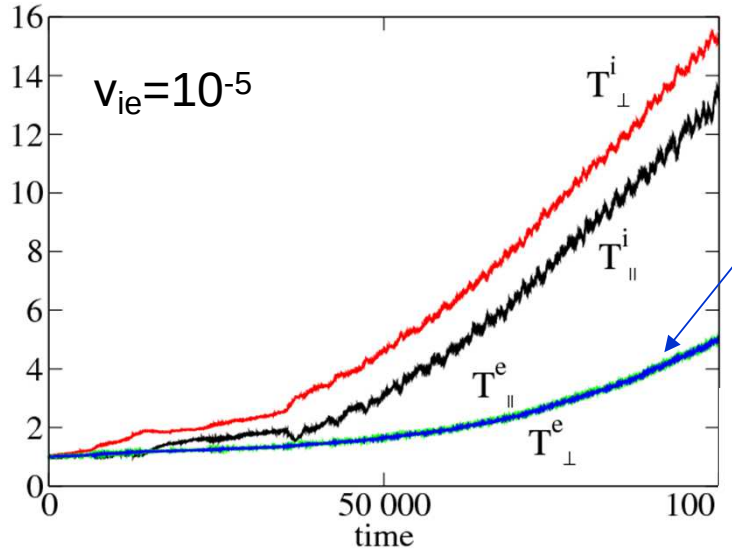

Equal parallel and perpendicular electron temperatures.

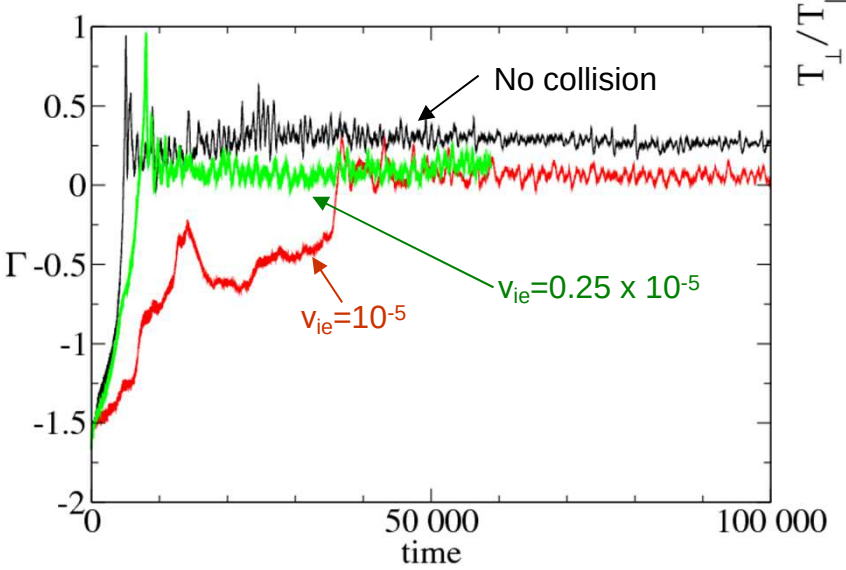

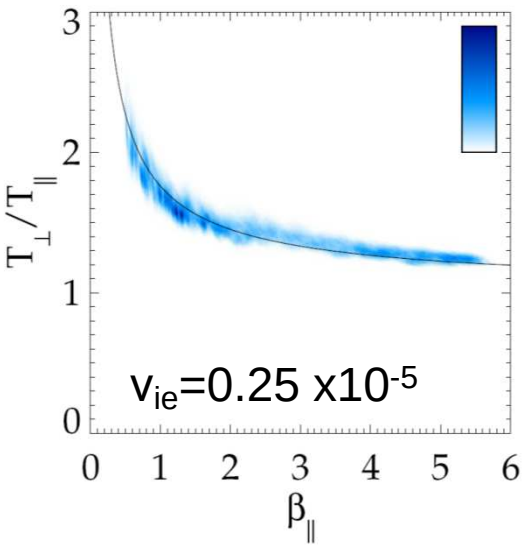

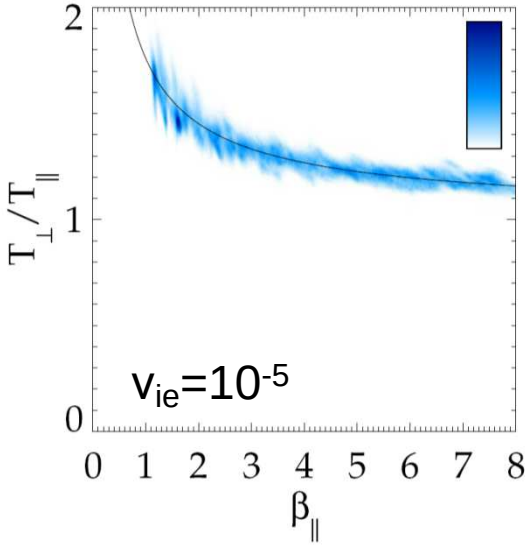

With collisions, points characterizing the state of the system follow the threshold curve

With collisions, smaller distance to threshold.

Conclusions

In situations where the distribution function is not too far from a Maxwellian, it is possible to recourse to fluid models to describe low frequency phenomena.

In order to address small-scale phenomena in directions quasi-perpendicular to the ambient magnetic field in plasmas with temperature anisotropy, fluid models should contain a minimum amount of complexity:

- equations for the fluid hierarchy up to heat fluxes
- finite Larmor radius corrections with the correct dependency on wave numbers (Bessel functions)
- closure that retains Landau damping for both ions and electrons.

This FLR-Landau fluid model can capture plasma heating, an issue of importance in accretion disks and in the intra-cluster medium, where the micro-instabilities have large-scale consequences.

Three-dimensional simulations of the full model are coming soon and should shed light on the transition of the KAW cascade at the ion scale.